ACS Catalysis

pubs.acs.org/acscatalysis Research Article

# Homo- and Cross-Coupling of Phenylacetylenes and α-Hydroxyacetylenes Catalyzed by a Square-Planar Rhodium Monohydride

Laura A. de las Heras, Miguel A. Esteruelas,* Montserrat Oliván, and Enrique Oñate

Cite This: ACS Catal. 2024, 14, 8389−8404 Read Online

ACCESS | Metrics & More | Article Recommendations | Supporting Information

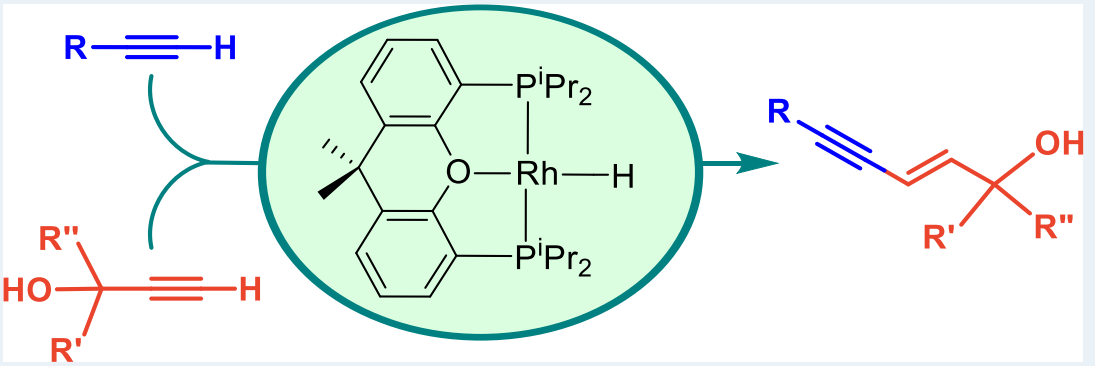


**ABSTRACT:** The C−C triple bond of phenylacetylene undergoes the *anti*-Markovnikov addition of the Rh−H bond of RhH{$\kappa^3$-*P,O,P*-[xant(P$^i$Pr$_2$)$_2$]} (**1**; xant(P$^i$Pr$_2$)$_2$ = 9,9-dimethyl-4,5-bis(diisopropylphosphino)xanthene) to give Rh{(*E*)−CH═CHPh}{$\kappa^3$-*P,O,P*-[xant(P$^i$Pr$_2$)$_2$]} (**2**), which reacts with a second alkyne molecule to produce Rh(C≡CPh){$\kappa^3$-*P,O,P*-[xant(P$^i$Pr$_2$)$_2$]} (**3**) and styrene before the transformation from **1** to **2** is complete. The metal center of **3** undergoes the oxidative addition of the C(sp)−H bond of another alkyne molecule to produce RhH(C≡CPh)$_2${$\kappa^3$-*P,O,P*-[xant(P$^i$Pr$_2$)$_2$]} (**4**), which also reacts with more phenylacetylene before completing the transformation from **3** to **4**. The reaction leads to Rh{(*E*)−CH═CHPh}(C≡CPh)$_2${$\kappa^3$-*P,O,P*-[xant(P$^i$Pr$_2$)$_2$]} (**5**), which reductively eliminates (*E*)-1,4-diphenyl-1-buten-3-yne to regenerate **3**. Complexes **3**, **4**, and **5** constitute a cycle for head-to-head dimerization of phenylacetylene. Consequently, complex **1** promotes the catalytic homocoupling of terminal alkynes to (*E*)-enynes, including the dimerization of α-hydroxyacetylenes to (*E*)-enyne-diols. The rate-determining step of the couplings depends on the nature of the alkyne, being the insertion of the C−C triple bond into the Rh−H bond of a bis(acetylide)-rhodium(III)-hydride intermediate for phenylacetylenes and the reductive elimination of the product (*E*)-enyne-diol for α-hydroxyacetylenes. In support of the latter, complex Rh{(*E*)−CH═CHC(OH)Ph$_2$}{C≡CC(OH)Ph$_2$}$_2${$\kappa^3$-*P,O,P*-[xant(P$^i$Pr$_2$)$_2$]} (**6**) has been isolated and characterized by X-ray diffraction analysis. Complex **1** also effectively promotes the formation of compounds of the type (*E*)-5-phenyl-2-penten-4-yn-1-ol, by cross-coupling between phenylacetylenes and α-hydroxyacetylenes. These reactions take place through two cycles similar to the cycle that produces the homocouplings, the rate-determining step being the reductive elimination of (*E*)-enyn-ol for both. The catalytic performance of **1** provides good efficiency in homocoupling and cross-coupling reactions involving progestin-type compounds such as ethisterone.

**KEYWORDS:** *rhodium, hydride, alkyne, homocoupling, cross-coupling*

## INTRODUCTION

Diastereoselective coupling of terminal alkynes catalyzed by transition metal complexes is a direct and atom-economical procedure to form 1,3-enynes, which are important building blocks in organic synthesis.[1] However, it is a great challenge; in the simplest case involving two molecules of the same alkyne, homocoupling, dimerization can be head-to-head or head-to-tail.[2] The first type of coupling is able of generating (*E*)- and (*Z*)-1,2,3-butatrienes[3] and (*E*)- and (*Z*)-1,4-disubstituted-1-buten-3-ynes, while 2,4-disubstituted-1-buten-3-ynes are formed via the second. Thus, the reactions can give two butatrienes in addition to three 1,3-enynes (Scheme 1), existing a limited number of catalysts capable of reaching high selectivity in the formation of only one of the 1,3-enynes.[2]

Received: January 12, 2024
Revised: April 26, 2024
Accepted: May 3, 2024
Published: May 14, 2024






https://doi.org/10.1021/acscatal.4c00264
ACS Catal. 2024, 14, 8389−8404

**Scheme 1. Homocoupling of Alkynes**

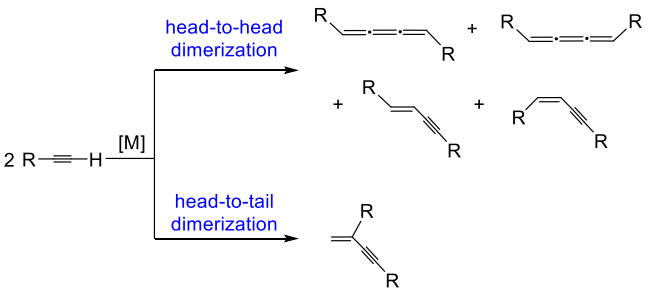


The elementary steps for the dimerization to enynes are an insertion between two C(sp)−H-bond activations. The insertion step decides the stereochemistry of the product, whereas the heterolytic or homolytic character of the C(sp)−H bond rupture depends on the electronic nature of the catalyst precursor (Scheme 2). Electron-poor precursors promote heterolytic cleavage to produce an acetylide derivative. Subsequent insertion of the C−C triple bond of another alkyne molecule into the metal-acetylide bond leads to a $\eta^3$-butenynyl intermediate, which then reacts with a new alkyne molecule to give the dimer and regenerate the active acetylide species (**a** in Scheme 2).[4] In contrast, electron-rich precursors react by homolytic cleavage of the C(sp)−H bond, to give a hydride−metal−acetylide complex. This species inserts the C−C triple bond of a new alkyne molecule, into the metal-hydride bond, to generate an alkenyl-metal-acetylide intermediate. In the presence of more alkyne, this intermediate undergoes reductive elimination of the dimer, regenerating the key hydride-metal-acetylide species (**b** in Scheme 2).[5]

The $\alpha$-hydroxyacetylenes occupy a prominent position among the alkyne substrates. They are present as an additional chemical function in several progestins, including norethindrone, norgestrel, ethisterone, and related steroid-containing molecules;[6] relevant biologically active compounds, with interesting pharmaceutical applications.[7] In addition, the dimerization products of these substrates, enyne-diols, are a direct pathway for the synthesis of enol ethers and a wide variety of oxygen-containing heterocycles.[8] This class of substrates has surprisingly received very little attention, with reactions being limited to a few simple substrates. Rhodium catalysts promote the preferential formation of head-to-head (*E*)-products,[9] whereas palladium precursors favor head-to-tail dimers.[10] In contrast to the rhodium and palladium complexes, osmium(IV)-polyhydride $OsH_3(SiEt_3)\{\kappa^3\text{-}P,O,P\text{-}[xant(P^iPr_2)_2]\}$ (xant-$(P^iPr_2)_2$ = 9,9-dimethyl-4,5-bis(diisopropylphosphino)-xanthene) promotes the head-to-head dimerization of 1,1-diphenyl-2-propyn-1-ol to the *Z*-enyne-diol. Under the reaction conditions, the latter is not stable and evolves to a furanol, which results from the addition of the hydroxy group in 1-position to the C−C triple bond.[11]

Cross-coupling between different terminal alkynes represents a significant increase in the level of difficulty. Besides the problem of the formation of different stereoisomers, each alkyne molecule must play a specific role; one of them acting as a hydrogen donor and the other as a hydrogen acceptor. Furthermore, the cross-coupling is competitive with the homocoupling of both alkynes, all three couplings taking place through similar mechanisms. Thus, cross-couplings must have a lower activation energy than homocouplings to proceed successfully.[12] To bypass these difficulties, one of the alkynes is often used in excess over the other.[4c,13] $\alpha$-Hydroxyacetylenes act as hydrogen acceptors in these reactions. Therefore, they are involved in the insertion step, which generally gives a M−CH═C(C≡CR)C(OH)$R'_2$ intermediate (**a** in Scheme 2) or is of the

**Scheme 2. Reaction Pathways for the Dimerization of Terminal Alkynes to 1,3-Enynes**

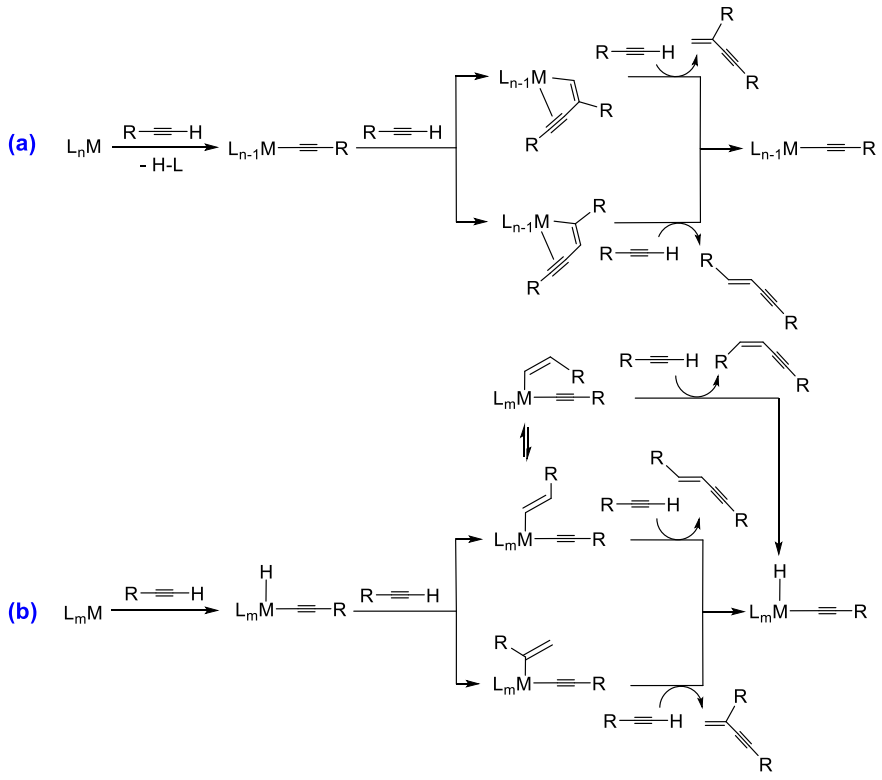




https://doi.org/10.1021/acscatal.4c00264
ACS Catal. 2024, 14, 8389−8404

Markovnikov-type (**b** in Scheme 2). Thus, the main reaction product is usually a *gem*-stereoisomer,[14] with very few exceptions.[15] Shaughnessy and co-workers reported a palladacycle-promoted cross-coupling between propargyl alcohols, with a $sp^2$-hybridized substituent on the carbon atom at 1-position and phenylacetylene. In contrast to the common trend, the reactions produce (*E*)-5-phenyl-2-penten-4-yn-1-ol derivatives in 61−73% yield;[16] compounds of particular interest, as they can be used as precursors of class NNC 61-4655 candidate drugs for type-2 diabetes.[17]

Pincer ligands have gained prominence in catalysis in the last two decades. The robustness provided to catalysts by the strong tridentate coordination of the pincer, which is highly desirable to withstand harsh reaction conditions, was initially argued as the main reason for its rapid implementation. Catalysts stabilized by pincer ligands are, however, much more, since they are demonstrating reactivity adapted to the requirements of certain transformations or behaviors in accordance with certain applications;[18] abilities related to the properties of the pincer, including coordinative flexibility and hemilability. Diphosphine xant$(P^iPr_2)_2$[19] significantly improves the capabilities of classical *P,O,P*-ligands.[20] It shows a greater tendency to coordinate as a pincer,[21] providing robust catalysts.[22] Despite this, its oxygen atom is hemilabile, which allows for bidentate coordination.[23] In addition, it acts with a wide variety of coordination forms, including $\kappa^3$-*P,O,P-mer* and *-fac*, and $\kappa^2$-*P,P-cis* and *-trans*.[24] As a result, efficient ruthenium,[25] osmium,[11,26] rhodium,[27] and iridium[28] catalysts stabilized by this diphosphine have been reported for a variety of organic and inorganic reactions. Among them, the monohydride RhH{$\kappa^3$-*P,O,P*-[xant$(P^iPr_2)_2$]} occupies a distinguished position; it catalyzes the borylation of arenes,[29] the deuteration of boranes and hydrides of group 14 elements,[30] the ammonia borane dehydrogenation,[31] and the dehydropolymerization of amine-boranes.[32]

The versatility of this monohydride led us to explore its catalytic performance for the coupling of terminal alkynes. This paper demonstrates that monohydride RhH{$\kappa^3$-*P,O,P*-[xant-$(P^iPr_2)_2$]} is an efficient catalyst precursor for the homocoupling of a wide variety of terminal alkynes and $\alpha$-hydroxyacetylenes, to selectively give (*E*)-enyne and (*E*)-enyne-diols, respectively. This complex also promotes cross-coupling between phenylacetylenes and $\alpha$-hydroxyacetylenes with a secondary or tertiary alcohol function. The scope of cross-coupling includes ethisterone and leads to a broader range of (*E*)-5-phenyl-2-penten-4-yn-1-ol derivatives than that previously reported with the Shaughnessy's palladacycle, with better selectivity and higher yields. In addition, the coupling mechanism is established through the characterization of the key catalytic intermediates and DFT calculations, and the reason for the observed selectivity is also analyzed.

## RESULTS AND DISCUSSION

**Homocouplings.** One of the most common reactions of unsaturated transition metal monohydride complexes is the addition of the M−H bond to the C−C triple bond of an alkyne to produce metal-alkenyl derivatives. The C−C double bond of the alkenyl ligand rarely prevents for the electron deficiency of the metal when it is a 4d element, in contrast to what is observed for the 5d derivatives of this class. Unsaturated complexes of platinum group metals also have a remarkable ability to activate $\sigma$-bonds; activation of the C(sp)−H bond of terminal alkynes being particularly easy. The behavior of monohydride RhH{$\kappa^3$-*P,O,P*-[xant$(P^iPr_2)_2$]} (**1**) toward phenylacetylene is consistent with this (Scheme 3).

**Scheme 3. Reaction of 1 with Terminal Alkynes Showing the Spectroscopically Detected and Isolated Species**

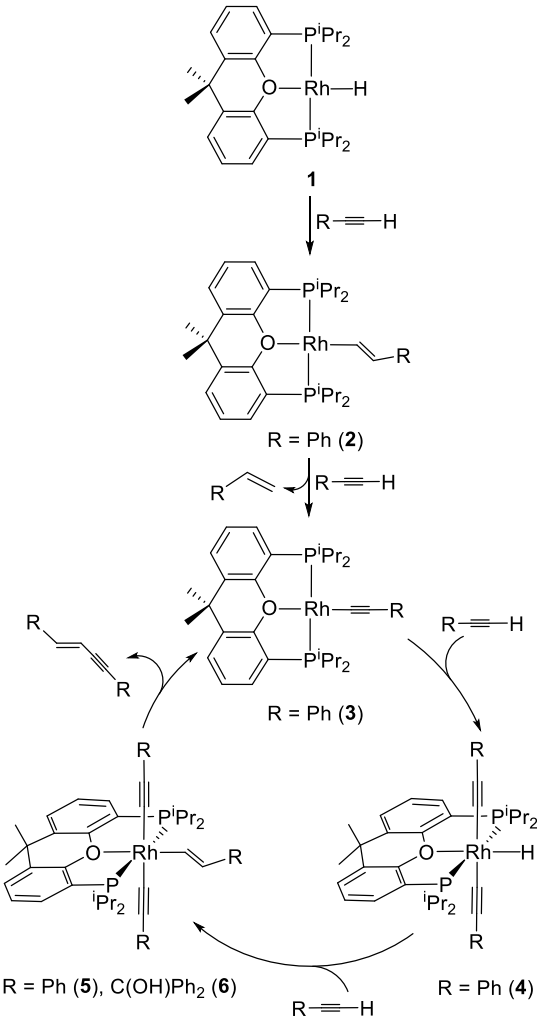


The C−C triple bond of phenylacetylene undergoes the *anti*-Markovnikov addition of the Rh−H bond of **1** to give the alkenyl derivative Rh{(*E*)−CH═CHPh}{$\kappa^3$-*P,O,P*-[xant$(P^iPr_2)_2$]} (**2**). However, the latter reacts with a second alkyne molecule before the transformation from **1** to **2** is completed. The reaction leads to the acetylide compound Rh(C≡CPh){$\kappa^3$-*P,O,P*-[xant$(P^iPr_2)_2$]} (**3**) and styrene, as a result of the oxidative addition of the C(sp)-H bond of phenylacetylene to the rhodium center of **2** and the subsequent reductive elimination of the olefin. Thus, the addition of less than 2.0 equiv of alkyne to solutions of **1**, in benzene-$d_6$, at room temperature leads to mixtures of **2** and **3**, together with styrene in the same molar quantity as **3**. The presence of **2** in the mixtures is strongly supported by a doublet of triplets of doublets ($^2J_{H-Rh}$ = 3 Hz, $^3J_{H-P}$ = 6 Hz, $^3J_{H-H}$ = 17 Hz) at 9.90 ppm in the $^1$H NMR spectrum, characteristic resonance for the RhCH-hydrogen atom (Figure S1), and a doublet ($^1J_{P-Rh}$ = 176 Hz) at 38.6 ppm in the $^{31}$P{$^1$H} NMR spectrum (Figure S2). Complex **3** was isolated as a white solid in almost quantitative yield by addition of 2.5 equiv of alkyne to solutions of **1**, in pentane, at room temperature. The presence of the acetylide ligand is supported


https://doi.org/10.1021/acscatal.4c00264
ACS Catal. 2024, 14, 8389−8404

by the IR and the $^{13}C\{^1H\}$ NMR spectrum, in benzene-$d_6$, at room temperature. The first contains a characteristic $\nu(C{\equiv}C)$ band at 2088 $cm^{-1}$, whereas the second shows two doublets of triplets at 123.8 ($^2J_{C-Rh}$ = 20.1 Hz, $^3J_{C-P}$ = 4.2 Hz) and 110.0 ($^1J_{C-Rh}$ = 62.0 Hz, $^2J_{C-P}$ = 19.2 Hz) ppm due to the $C_\beta$ and $C_\alpha$ atoms of the C-donor ligand, respectively. A doublet ($^1J_{P-Rh}$ = 152 Hz) at 45.5 ppm in the $^{31}P\{^1H\}$ NMR spectrum is another noticeable feature of this compound.

The metal center of **3** is coordinatively unsaturated, like that of **2**, and, in agreement with the latter, it undergoes oxidative addition of the C(sp)−H bond of a new alkyne molecule to produce the monohydride-rhodium(III) derivative RhH(C≡CPh)$_2${$\kappa^3$-*P,O,P*-[xant(P$^i$Pr$_2$)$_2$]} (**4**). Complex **4** is also unstable in the presence of the alkyne. In spite of its saturated character, it reacts with more phenylacetylene before the transformation from **3** to **4** is completed. The reaction leads to the alkenyl-rhodium(III)-bis(acetylide) species Rh{(*E*)−CH═CHPh}-(C≡CPh)$_2${$\kappa^3$-*P,O,P*-[xant(P$^i$Pr$_2$)$_2$]} (**5**), as a consequence of the *anti*-Markovnikov insertion of the C−C triple bond of the alkyne in the Rh−H bond. The hemilabile character of the diphosphine oxygen atom and the coordinative flexibility of this ligand allow coordination of the alkyne and their subsequent migratory insertion. As a result of both reactions, the addition of approximately 11 equiv of phenylacetylene to the solutions of **3**, in benzene-$d_6$, at room temperature generates a mixture of **3**, **4**, and **5** in a molar ratio of about 25:67:8 after 10−20 min (Figure S6). Spectroscopic identification features of **4** are a doublet of triplets ($^1J_{H-Rh}$ = 32.2 Hz, $^2J_{H-P}$ = 12.0 Hz) at −18.84 ppm, corresponding to the hydride ligand, in the $^1H$ NMR spectrum (Figure S7) and a doublet ($^1J_{P-Rh}$ = 100 Hz) at 54.4 ppm in the $^{31}P\{^1H\}$ NMR spectrum (Figure S6). The presence of **5** in the mixture is supported by a doublet of triplets of doublets ($^2J_{H-Rh}$ = 1.2 Hz, $^3J_{H-P}$ = 2.1 Hz, $^3J_{H-H}$ = 14.3 Hz) at 8.58 ppm, typical for a RhCH hydrogen atom (Figure S8), and a doublet with a characteristic P−Rh coupling constant for rhodium(III) of 100 Hz at 32.9 ppm in the $^{31}P\{^1H\}$ NMR spectrum (Figure S9). The mutually *trans* arrangement of the acetylide ligands in both compounds was inferred from the aliphatic resonances in the $^1H$ NMR spectra, which for each compound show two signals for the methyl groups of the diisopropylphosphine substituents and one signal for the methyl substituents of the central heterocycle. This signal pattern is consistent with the existence of a molecular plane of symmetry, which makes equivalent the two acetylide ligands, the isopropyl substituents of each P$^i$Pr$_2$ group, and the methyl substituents of the central heterocycle.

Complex **5** reductively eliminates (*E*)-1,4-diphenyl-1-buten-3-yne to regenerate **3**. Therefore, complexes **3**, **4**, and **5** constitute a stoichiometric cycle for head-to-head (*E*)-dimerization of phenylacetylene. To obtain information on the catalytic performance of this cycle, we treated complex **3** with 20 equiv of alkyne, in benzene-$d_6$, at 80 °C. As expected, the selective formation of (*E*)-1,4-diphenyl-1-buten-3-yne was observed, in almost quantitative yield (93%), after 10 h. Figure 1a shows the transformation profile, while Figure 1b provides the $^{31}P\{^1H\}$ NMR spectra of the solution as a function of time. The spectra show that the cycle generated is, of course, catalytic; complexes **3** and **4** are present in all the spectra and some of them also contain traces of **5**. A qualitative analysis of the variation of the concentration of the species observed over time also indicates that (i) the rhodium(I)-acetylide complex **3** is the organometallic species that initiates and recovers from catalysis. (ii) The monohydride-rhodium(III) derivative **4** is a catalytic intermediate, which is in equilibrium with **3**. (iii) Insertion of the

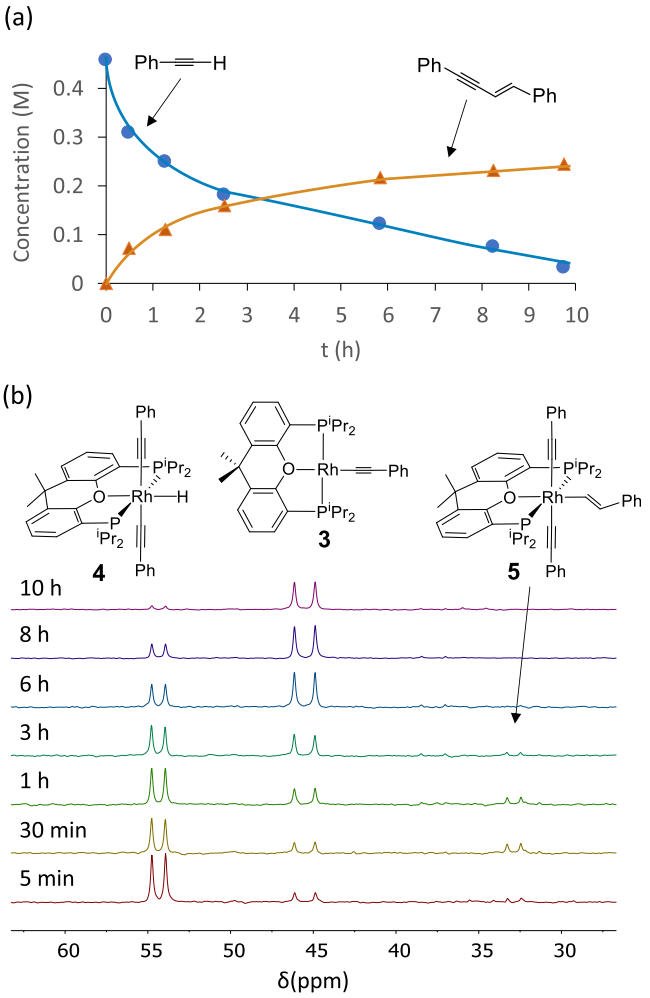


**Figure 1.** (a) Profile of the dimerization of phenylacetylene to (*E*)-1,4-diphenyl-1-buten-3-yne. (b) Stacked $^{31}P\{^1H\}$ NMR spectra showing the reaction of complex **3** with 20 equiv of phenylacetylene (benzene-$d_6$, 80 °C).

C−C triple bond of the alkyne into the Rh−H bond of **4** to give **5** is the rate-determining step of the catalysis, since complex **4** is the main metallic species for higher alkyne concentrations. (iv) The reductive elimination of the (*E*)-1,3-enyne is fast.

Having established the catalytic character of the cycle shown in Scheme 3, we decided to study the range of alkynes that can be coupled in a similar way. Scheme 3 indicates that each dimerization takes place through its own square-planar rhodium(I) acetylide derivative. These species result from the reaction of monohydride **1** with 2.0 equiv of alkyne. Therefore, they can be generated in the reaction by adding an additional 2.0 equiv of substrate. The use of 2.4 mol % of acetylide complex with regard to the total amount of alkyne, benzene, and 80 °C are appropriate catalytic conditions to perform the dimerization. Under these conditions, complex **1** is an efficient catalyst precursor to promote head-to-head dimerization of a variety of substituted phenylacetylenes, showing good tolerance to functional groups ($CF_3$, F, CN, OMe, and $NMe_2$). The corresponding (*E*)-1,3-enynes (**a$_4$**−**f$_4$**) are selectively obtained with a high yield (≈90%), after 22 h, in all cases. 2-Ethynyl-naphthalene, 2-methyl-1-buten-3-yne, 3-phenyl-1-propyne, and trimethylsilylacetylene also efficiently and selectively homo-couple to produce the respective (*E*)-1,3-enynes (**g$_4$**−**j$_4$**)


https://doi.org/10.1021/acscatal.4c00264
ACS Catal. 2024, 14, 8389−8404

(Scheme 4). In contrast, *tert*-butylacetylene does not give significant yields of dimer.

**Scheme 4. Homocoupling of Terminal Alkynes**[a]

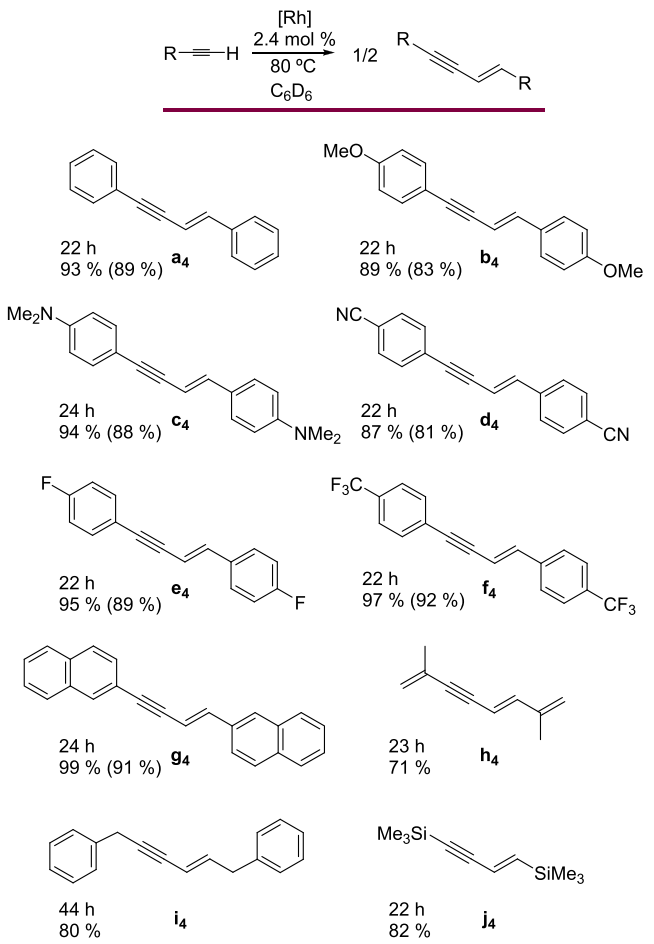


[a]Conditions: **1** (5 mg, 0.009 mmol), alkyne (0.38 mmol), and benzene-$d_6$ (0.4 mL). Yields were determined by $^1$H NMR using dioxane or 1,1,2,2-tetrachloroethane as internal standards; isolated yields are given in parentheses.

Tolerance of **1** to functional groups includes alcohols. This monohydride derivative is also an efficient catalyst precursor for the homocoupling of $\alpha$-hydroxyacetylenes having a secondary or tertiary alcohol function. Under the same conditions as those used in the dimerization of phenylacetylenes, it promotes head-to-head dimerization of a wide range of these substrates, including compounds with alkyl, phenyl, and vinyl substituents at the alcohol function. The coupling selectively generates (*E*)-enyne-diols $\mathbf{a_5}$-$\mathbf{i_5}$ (Scheme 5), in very high yields (80−90%). Preparation of nonreported compounds (*E*)-2,9-dimethyl-4-decen-6-yne-3,8-diol ($\mathbf{b_5}$), (*E*)-2,11-dimethyl-5-decen-7-yne-4,9-diol ($\mathbf{c_5}$), and (*E*)-3,8-dimethyl-1,4,9-decatrien-6-yne-3,8-diol ($\mathbf{d_5}$) and their characterizations should be highlighted.

The $^{31}$P{$^1$H} NMR spectra of the solution, in which the formation of (*E*)-1,1,6,6-tetraphenyl-2-hexen-4-yne-1,6-diol ($\mathbf{i_5}$) takes place, revealed that the ($\alpha$-hydroxyalkenyl)-rhodium(III)-bis($\alpha$-hydroxyacetylide) complex Rh{(*E*)−CH═CHC(OH)Ph$_2$}{C≡CC(OH)Ph$_2$}$_2${$\kappa^3$-*P,O,P*-[xant(P$^i$Pr$_2$)$_2$]} (**6**) is the main rhodium species in the reaction (Figure S10); the analogue of **5**. Its presence rests on a doublet ($^1J_{P-Rh}$ = 101.5 Hz) at 34.6 ppm. Complex **6** was obtained on a preparative scale as a

**Scheme 5. Homocoupling of $\alpha$-Hydroxyacetylenes**[a]

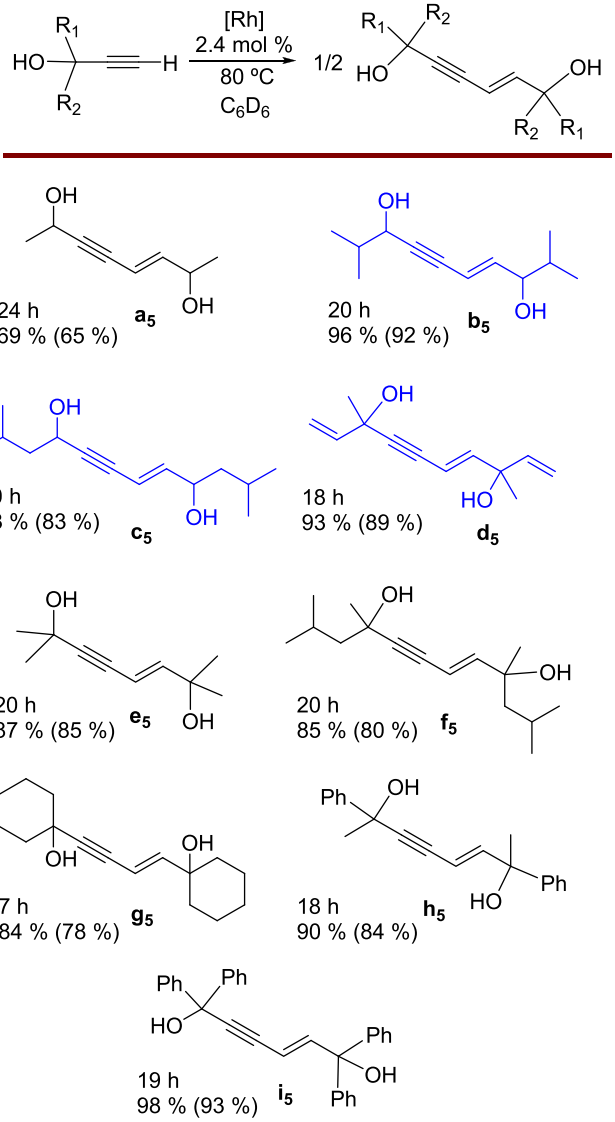


[a]Nonreported compounds in blue. Conditions: **1** (5 mg, 0.009 mmol), alkyne (0.38 mmol), and benzene-$d_6$ (0.4 mL). Yields were determined by $^1$H NMR using dioxane as internal standard; isolated yields are given in parentheses.

white solid, in 82% yield, by treating **1** with 4.0 equiv of 1,1-diphenyl-2-propyn-1-ol, in toluene, at room temperature. It was then characterized by X-ray diffraction analysis. The structure has two chemically equivalent but crystallographically independent molecules in the asymmetric unit; Figure 2 shows one of them. The coordination polyhedron around the rhodium(III) center is an octahedron, as befits a d$^6$ six-coordinate species. The ether-diphosphine coordinates *mer*, with angles P(1)−Rh(1)−P(2) of 163.18(11) and 161.65(12)°. In addition, the structure confirms the *trans* arrangement of the $\alpha$-hydroxyacetylide ligands, which form C(16)−Rh(1)−C(31) angles of 178.5(5)° and 177.2(4)°, and the *trans* arrangement of the $\alpha$-hydroxyalkenyl group to the etherdiphosphine oxygen atom (C(1)−Rh(1)−O(1) = 174.3(4) and 177.7(5)°). The $\alpha$-hydroxyalkenyl group shows an *E* stereochemistry at the C−C double bond, as expected for a concerted *anti*-Markovnikov addition of a Rh−H bond to the C−C triple bond of a terminal alkyne. The $^{13}$C{$^1$H} NMR spectrum in benzene-$d_6$ is consistent



https://doi.org/10.1021/acscatal.4c00264
ACS Catal. 2024, 14, 8389−8404

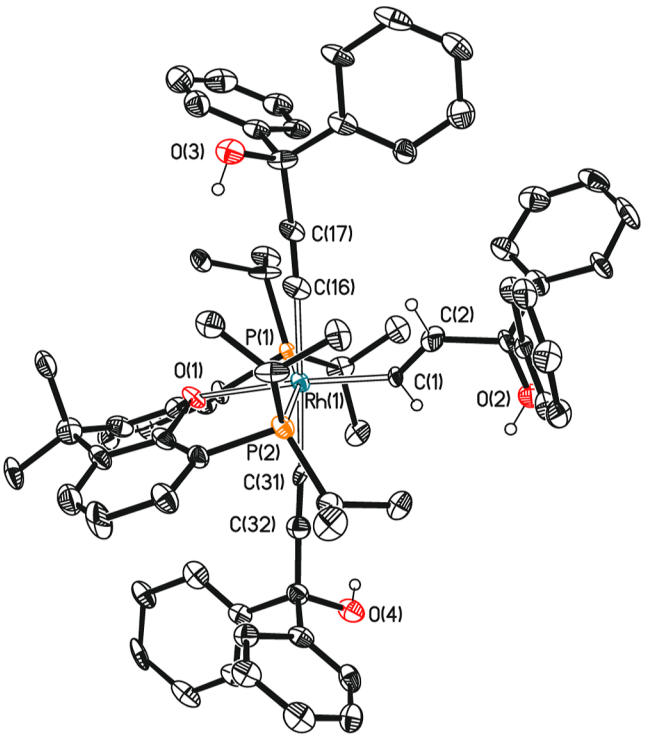


**Figure 2.** Molecular diagram of one of the two chemically equivalent but crystallographically independent molecules of complex **6** (displacement ellipsoids shown at 50% probability). All hydrogen atoms (except those of the vinyl and OH moieties) are omitted for clarity. Selected bond distances (Å) and angles (deg): Rh(1)−P(1) = 2.304(3), 2.320(3), Rh(1)−P(2) = 2.306(3), 2.304(3), Rh(1)−O(1) = 2.291(8), 2.278(8), Rh(1)−C(1) = 2.016(10), 2.014(11), Rh(1)−C(16) = 2.046(13), 2.012(11), Rh(1)−C(31) = 2.049(12), 2.050(12), C(1)−C(2) = 1.317(17), 1.310(17), C(16)−C(17) = 1.203(18), 1.207(17), C(31)−C(32) = 1.208(17), 1.215(17); P(1)−Rh(1)−P(2) = 163.18(11), 161.65(12), O(1)−Rh(1)−C(1) = 174.3(4), 177.7(4), C(16)−Rh(1)−C(31) = 178.5(5), 177.2(4).

with the presence of the $\alpha$-hydroxyacetylide and $\alpha$-hydroxyalkenyl ligands in the complex. The C(sp) carbon atoms of the equivalent $\alpha$-hydroxyacetylide groups give rise to doublets of triplets at 113.4 ($C_\alpha$, $^1J_{C-Rh}$ = 38.9 Hz, $^2J_{C-P}$ = 15.5 Hz) and 109.8 ($C_\beta$, $^1J_{C-Rh}$ = 3.0 Hz, $^2J_{C-P}$ = 0.8 Hz) ppm, while the C($sp^2$) atoms of the vinylic moiety of the $\alpha$-hydroxyalkenyl ligand generate a triplet ($C_\beta$, $^3J_{C-P}$ = 3.7 Hz) at 139.0 and a doublet of triplets ($C_\alpha$,$^1J_{C-Rh}$ = 34.1 Hz, $^2J_{C-P}$ = 9.9 Hz) at 129.7 ppm.

Complex **6** reductively eliminates (*E*)-1,1,6,6-tetraphenyl-2-hexen-4-yne-1,6-diol, in benzene-$d_6$, to produce the square planar derivative Rh{C≡CC(OH)$Ph_2$}{$\kappa^3$-*P,O,P*-[xant-($P^iPr_2$)$_2$]} (**7**; $\delta_{31P}$, 45.9 ppm; $^1J_{P-Rh}$ = 151.5 Hz); the analogue of **3**. This stoichiometric reaction and the presence of **6** in the catalytic solution as the main organometallic species suggest that the sequence of events for the dimerization of 1,1-diphenyl-2-propyn-1-ol is the same as for the dimerization of phenylacetylene, although the steps that determine the rate of both reactions are different. Unlike the dimerization of phenylacetylene, the rate-determining step for the dimerization of 1,1-diphenyl-2-propyn-1-ol is the reductive elimination of (*E*)-1,1,6,6-tetraphenyl-2-hexen-4-yne-1,6-diol. Accordingly, the activation parameters for the stoichiometric reductive elimination and for the catalytic reaction are the same; $\Delta H^{\neq}$ = 19.7 ± 1.2 kcal mol$^{-1}$, $\Delta S^{\neq}$ = −16.9 ± 3.5 cal$^{-1}$ K$^{-1}$ mol$^{-1}$, and $^{298}\Delta G^{\neq}$ = 24.7 ± 2.2 kcal mol$^{-1}$ (Figure 3).

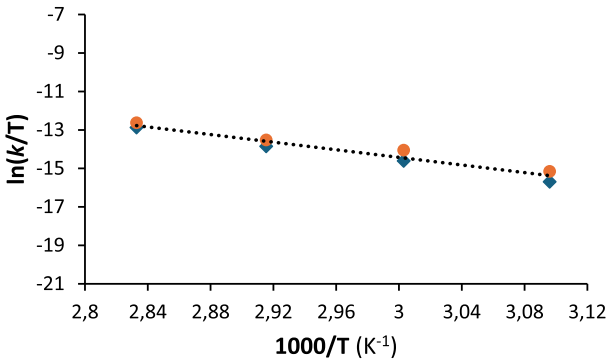


**Figure 3.** Eyring plot for the reductive elimination of (*E*)-1,1,6,6-tetraphenyl-2-hexen-4-yne-1,6-diol from **6** (blue squares) and for the catalytic dimerization of 1,1-diphenyl-2-propyn-1-ol (orange circles).

The DFT calculations (SMD-(toluene)-B3LYP-D3//SDD-(f)/6-31-G**) perfectly reproduce the cycle shown in Scheme 3 as well as the differences between phenylacetylenes and $\alpha$-hydroxyacetylenes, for our delight. The changes in free energy ($\Delta G$) were calculated at 298.15 K and 1 atm using phenylacetylene and 2-methyl-3-butyn-2-ol as alkyne models. Figure 4a shows the energy profile calculated for the homocoupling of the former, whereas Figure 4b shows that for the dimerization of the latter.

The oxidative addition of the C(sp)−H bond of the substrates to the respective rhodium(I)-acetylide catalysts **3** (Figure 4a) and **D** (Figure 4b) takes place in three steps. The first step involves the coordination of the C−C triple bond of the alkynes with the unsaturated metal center of the catalysts, initially leading to the $\pi$-alkyne intermediates **A** and **E**. In the second step, the metal center slides toward the C(sp)−H bond, to give **B** and **F**. In the third step, the $\sigma$-intermediates **B** and **F** undergo homolytic cleavage of the coordinated $\sigma$-bond. The generated rhodium(III) species **4** and **G** are approximately 1 kcal mol$^{-1}$ more stable than the respective rhodium(I)-acetylide compounds. This small difference in stability between the hydride-rhodium(III)-bis(acetylide) intermediates and the rhodium(I)-acetylide species is consistent with the coexistence of both in equilibrium, as revealed by the $^{31}P\{^1H\}$ NMR spectra shown in Figure 1b. The oxidative additions must overcome a maximum barrier of approximately 21 kcal mol$^{-1}$, which corresponds to the sliding of the metal center from the C−C triple bond to the $\sigma$−C−H bond.

The insertions of the C−C triple bond of alkynes into the Rh−H bond of the hydride-rhodium(III)-bis(acetylide) intermediates **4** and **G** to produce **5** and **H**, respectively, are concerted and occur throughout the typical transition states of four centers. Just as the C−C triple bond of the alkyne approaches the saturated metal center, the oxygen atom of diphosphine separates from the rhodium atom. In the transition states (Figure 5), the pincer ether-diphosphine becomes bidentate, acting with P−Rh−P angles of 117.1° in $\mathbf{TS_{4-5}}$ and 114.2° in $\mathbf{TS_{G-H}}$. Although $\mathbf{TS_{4-5}}$ and $\mathbf{TS_{G-H}}$ may superficially appear similar, there is a major difference in the barriers of the insertion process; while $\mathbf{TS_{4-5}}$ lies at 31.7 kcal mol$^{-1}$ over **4**, $\mathbf{TS_{G-H}}$ is only 20.2 kcal mol$^{-1}$ over **G**. The reason for such a surprising difference seems to be an electrostatic interaction between the oxygen atom of $\alpha$-hydroxyacetylene and the weakly


https://doi.org/10.1021/acscatal.4c00264
ACS Catal. 2024, 14, 8389−8404

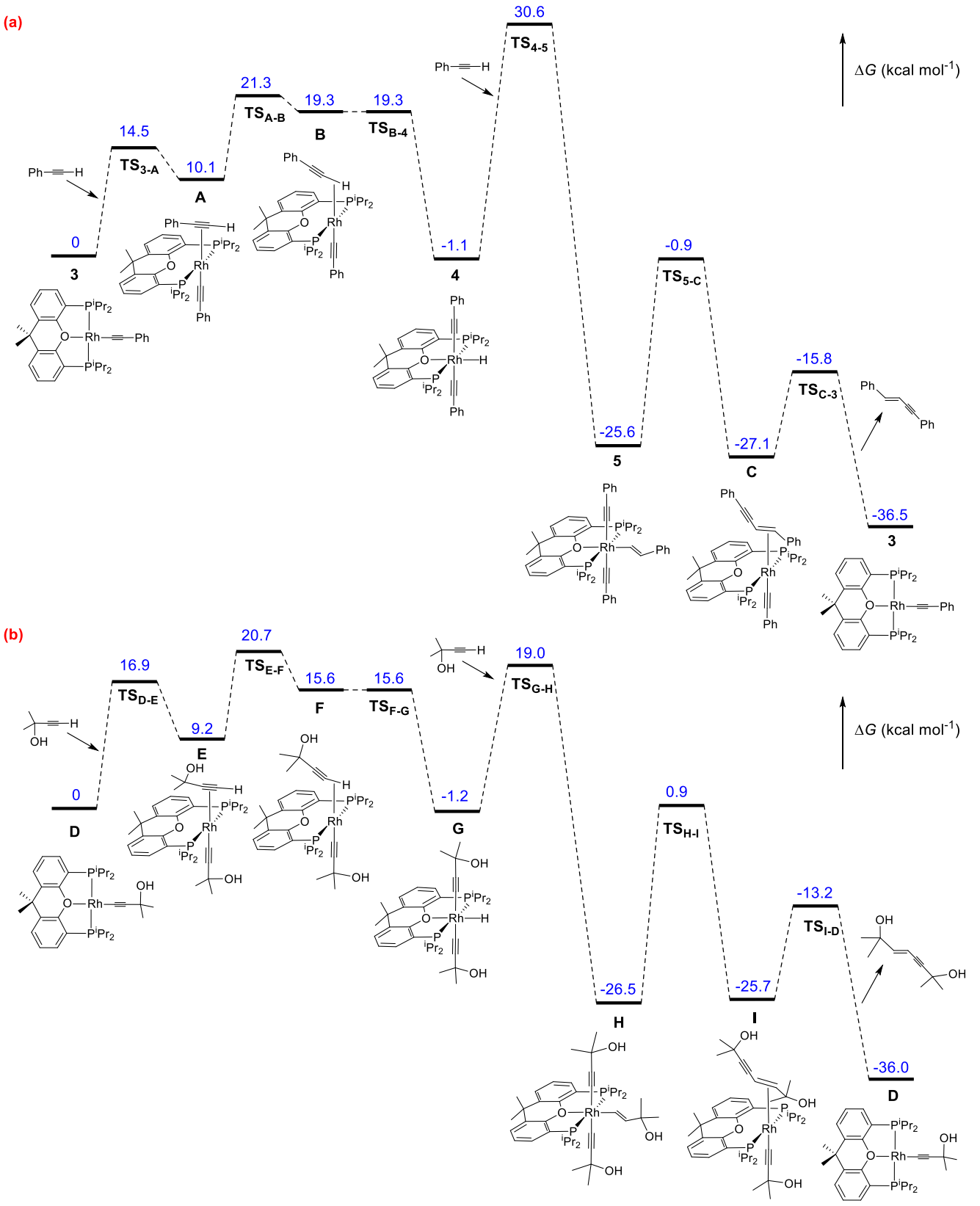


**Figure 4.** Computed energy profile ($\Delta G$, in kcal mol$^{-1}$) for the homocoupling of phenylacetylene (a) and 2-methyl-3-butyn-2-ol (b).

acidic hydride, which stabilizes $\mathbf{TS_{G\text{-}H}}$ with respect to $\mathbf{TS_{4-5}}$. The electrostatic character of the interaction in $\mathbf{TS_{G\text{-}H}}$ is supported by the hydride-oxygen separation of 2.311 Å, which is shorter than the sum of the van der Waals radii of hydrogen and oxygen ($r_{vdw}$(H) = 1.20 Å, $r_{vdw}$(O) = 1.52 Å),[33] and the Mulliken and NBO charges of the hydride (+0.067 and +0.096) and the oxygen atom of the $\alpha$-hydroxyacetylene (−0.514 and −0.760).



https://doi.org/10.1021/acscatal.4c00264
ACS Catal. 2024, 14, 8389−8404

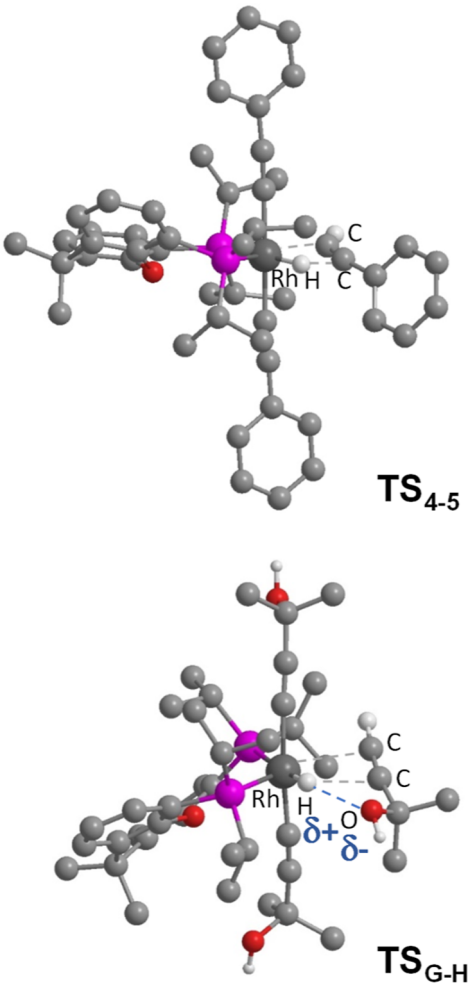


**Figure 5.** Transition states for the insertion of phenylacetylene (top) and 2-methyl-3-butyn-2-ol (bottom) into the Rh−H bond of the hydride-rhodium(III)-bis(acetylide) intermediates **4** and **G**. Hydrogens (except the hydrides, the OH and the C(sp)−H protons of the alkyne) are omitted for clarity.

Intermediates **5** and **H** evolve by reductive coupling of the alkenyl group and one of the acetylide ligands to give the enyne derivatives **C** and **I**, which release the coupled fragments to close the cycle. Reductive eliminations present similar barriers; 24.7 kcal $mol^{-1}$ for the dimerization of phenylacetylene and 27.4 kcal $mol^{-1}$ for the formation of enyne-diol. The contextualization of these values in the respective catalytic sequences indicates that the rate-determining dimerization step depends on the nature of the alkyne, although the steps required for both catalysis are similar, as expected based on the experimental results. The insertion of the C−C bond of the alkyne into the Rh−H bond of **4** is the rate-determining step for the dimerization of phenylacetylene. However, the reductive elimination of enyne-diol from the intermediate ($\alpha$-hydroxyalkenyl)-rhodium(III)-bis($\alpha$-hydroxyacetylide) **H** is the rate-determining step for the homocoupling of $\alpha$-hydroxyacetylene. Because the barrier for insertion of the C−C bond of phenylacetylene into the Rh−H bond of **4** is higher than that for the reductive elimination of enyne-diol from the ($\alpha$-hydroxyalkenyl)-rhodium(III)-bis($\alpha$-hydroxyacetylide) **H** intermediate, 2-methyl-3-butyn-2-ol homocoupling is faster than phenylacetylene homocoupling (Figure S115).

**Cross-Coupling of Phenylacetylenes and $\alpha$-Hydroxyacetylenes.** Complex **1** is also an efficient catalyst precursor for the formation of a variety of enyn-ols of the (*E*)-5-phenyl-2-penten-4-yn-1-ol type, by cross-coupling between phenylacetylenes and $\alpha$-hydroxyacetylenes and trimethylsilyl-related derivatives resulting from the use of trimethylsilylacetylene instead of arylacetylenes. Phenylacetylenes include substrates with MeO, CN, and $CF_3$ substituents on the phenyl group, while $\alpha$-hydroxyacetylenes are substituted terminal alkynes with secondary and tertiary alcohol functions that result from the presence of alkyl, phenyl, or vinyl substituents. The reactions were carried out in benzene, at 80 °C, with equimolar amounts of substrates, using 5 mol % of precursor with respect to both alkynes. Products $\mathbf{a_6}$−$\mathbf{m_6}$ were formed with yields of 80−90%, after 24 h. The yields are independent of the substituent of the C−C triple bonds, including the secondary or tertiary character of the alcohol, and the alkyl, phenyl, or vinyl nature of the alcohol substituents (Scheme 6). The efficiency of **1** is higher than that reported for Shaughnessy's palladacycle in the cross-coupling between phenylacetylenes and $\alpha$-hydroxyacetylenes, with primary and secondary alcohol functions, since our yields

**Scheme 6. Cross-Coupling of Phenylacetylenes and $\alpha$-Hydroxyacetylenes**[a]

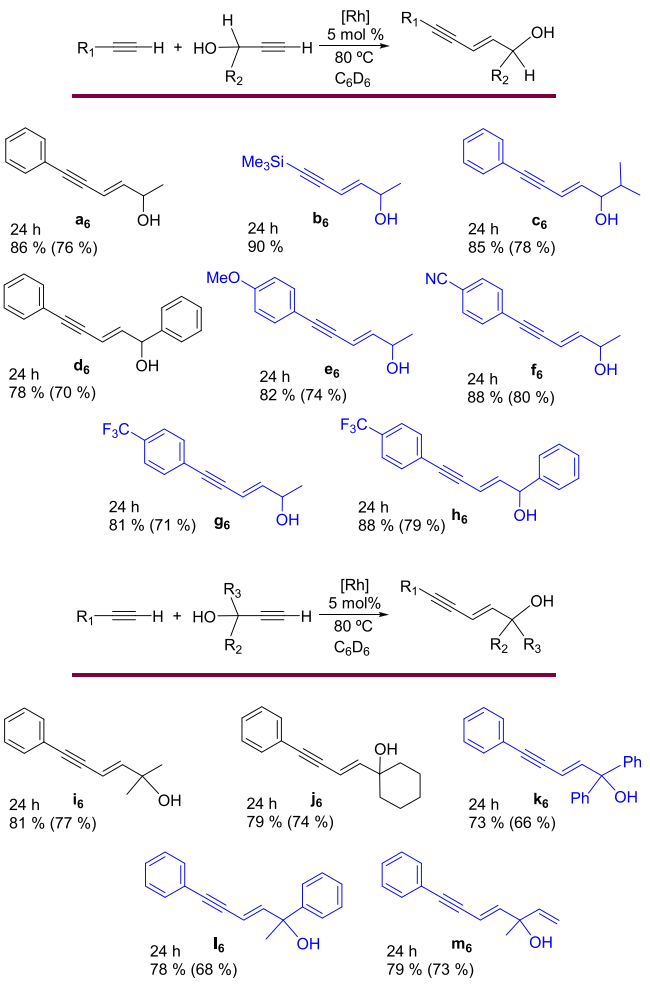


[a]Nonreported compounds in blue. Conditions: **1** (5 mg, 0.009 mmol), 0.19 mmol of each alkyne, and benzene-$d_6$ (0.4 mL). Yields were determined by $^1$H NMR using dioxane as internal standard; isolated yields are given in parentheses.



https://doi.org/10.1021/acscatal.4c00264
ACS Catal. 2024, 14, 8389−8404

**Scheme 7. Plausible Mechanisms for the Formation of Cross-Coupling Products between a Phenylacetylene and an α-Hydroxyacetylene**

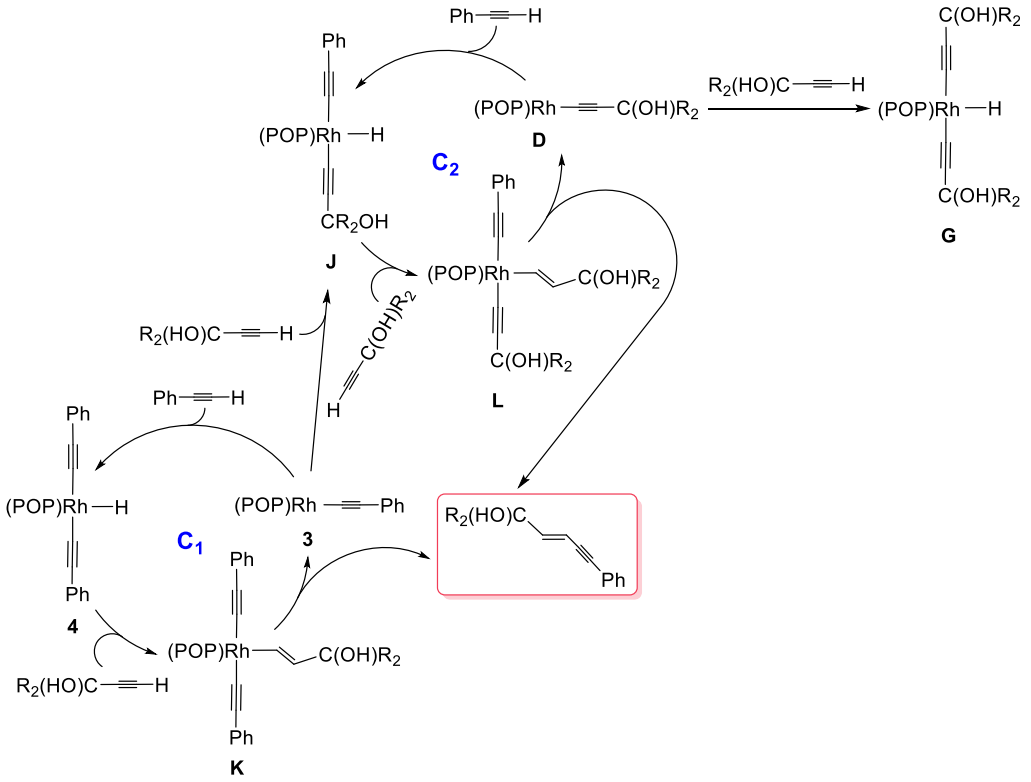


are higher. Furthermore, it should be noted that the Shaughnessy reactions were performed using an excess of α-hydroxyacetylene, between 2.5 and 5 equiv,[16] unlike our reactions.

Reaction crudes contain small amounts of homocoupling dimers. However, the (*E*)-5-phenyl-2-penten-4-yn-1-ols products were easily separated from these byproducts, by preparative thin-layer chromatography on silica gel, since their significantly different polarities. Thus, this catalysis is an efficient procedure of organic synthesis that allowed us to characterize five new (*E*)-5-phenyl-2-penten-4-yn-1-ols with a secondary alcohol function, three with a tertiary one, and $\mathbf{b}_6$. The new (*E*)-5-phenyl-2-penten-4-yn-1-ol derivatives include $\mathbf{c}_6$, $\mathbf{e}_6$–$\mathbf{h}_6$, and $\mathbf{k}_6$–$\mathbf{m}_6$. Compounds (*E*)-1,5-diphenyl-2-penten-4-yn-1-ol ($\mathbf{d}_6$) and (*E*)-6-phenyl-3-hexen-5-yn-2-ol ($\mathbf{a}_6$), which carry a secondary alcohol function, are known. The first of these is often used as a synthetic intermediate; it is generated by treatment of 5-phenyl-2-penten-4-ynoic acid ethyl ester with diisobutylaluminum hydride and is used immediately for subsequent reactions.[34] The second, the methyl counterpart, was prepared as a mixture of *E* and *Z* stereoisomers, by acid-catalyzed rearrangement of 1-phenyl-4-hexen-1-yn-3-ol. The latter is obtained from the reaction of 2-buten-1-al with lithium phenylacetylide.[35] However, a more appropriate procedure is the selective catalytic reduction of the carbonyl group of 6-phenyl-3-hexen-5-yn-2-one.[36] Also known are the compounds (*E*)-2-methyl-6-phenyl-3-hexen-5-yn-2-ol ($\mathbf{i}_6$) and (*E*)-1-(4-phenyl-1-buten-3-yn-1-yl)-1-cyclohexanol ($\mathbf{j}_6$), which have a tertiary alcohol function. They were prepared as now, by rhodium-catalyzed cross-coupling between phenylacetylene and the corresponding alkynol, but in much lower yields, >40%.[9a,14b]

Scheme 7 rationalizes the formation of products of the type (*E*)-5-phenyl-2-penten-4-yn-1-ol, by cross-coupling between a phenylacetylene and a α-hydroxyacetylene, based on the elementary steps of Scheme 3. Because there are two different alkynes involved in the reaction, two different rhodium(I)-acetylide species can be formed; **3** and an analogous α-hydroxyacetylide **D**. Oxidative addition of the C(sp)–H bond of both alkynes to the metal center of these species should lead to the bis(acetylide)-rhodium(III)-hydride derivatives **4**, **G**, and **J**. The roles of the alkynes in the cross-coupling process are predetermined; α-hydroxyacetylene acts as a hydrogen acceptor, while phenylacetylene is the hydrogen donor. Therefore, the insertions of the C–C triple bond of α-hydroxyacetylene into the Rh–H bond of **4** and **J** are the only productive additions among the possible ones and define the $C_1$ and $C_2$ cycles responsible for the formation of the heterocoupling products. Such insertions provide intermediates **K** and **L**, which are related compounds to **5** and **6** but heteroleptic in nature. The addition of the Rh–H bond of **4** and **J** to the C–C triple bond of the α-hydroxyacetylene must be faster than the insertion of the C–C triple bond of phenylacetylene into the Rh–H bond of **4**, since the latter is the rate-determining step of homocoupling of phenylacetylene. Once **K** and **L** are formed, they should undergo reductive elimination of the cross-coupling product. Elimination at **K** would regenerate **3**, while elimination at **L** would produce **D**. They are the rate-determining step of the cycles $C_1$ and $C_2$ and, as previously mentioned, must also be faster than the rate-determining steps of both homocouplings; the above-mentioned insertion of the C–C triple bond of phenylacetylene in the Rh–H bond of **4** and the reductive elimination of (*E*)-enyne-diol from **H**. The $^{31}P\{^1H\}$ NMR spectra of the solutions, in which the cross-coupling products are formed, recorded during the reactions are consistent with this. They show three doublets between 36 and 31 ppm (Figure S14); the region of the spectrum where **5** and **6** are observed. One of them corresponds


https://doi.org/10.1021/acscatal.4c00264
ACS Catal. 2024, 14, 8389–8404

to **H**,[37] which is responsible for the formation of the observed small amounts of dimer from α-hydroxyacetylene homocoupling, whereas the other two are due to **K** and **L**. Thus, the homocoupling byproducts are generated in two different phases of the cross-coupling reaction. α-Hydroxyacetylene homocoupling is a competitive reaction with cross-coupling, while phenylacetylene homocoupling only occurs when cross-coupling is complete. As a consequence of the loss of a small amount of α-hydroxyacetylene in competitive homocoupling, a small amount of phenylacetylene remains, which undergoes dimerization. Consistently, the $^{31}P\{^{1}H\}$ NMR spectra of solutions corresponding to reactions involving unsubstituted phenylacetylene show the presence of **3**, at the end of cross-coupling (Figure S14). DFT calculations on cycles $C_1$ and $C_2$ reproduce everything mentioned above.

Figure 6 shows the energy profile for the formation of **K**, by insertion of the C−C triple bond of the α-hydroxyacetylene into the R−H bond of **4**, and the release of the heterocoupling product, according to the $C_1$ cycle. The insertion of the C−C triple bond of α-hydroxyacetylene in the Rh−H bond of **4** must overcome an activation energy of 21.0 kcal mol$^{-1}$, similar to that observed for the same insertion in the Rh−H bond of the species bis(α-hydroxyacetylide) **G**. The transition states of both insertions are also similar; the ether-diphosphine coordinates in a bidentate manner, with a P−Rh−P bite angle of 114.0°, whereas the hydride and the oxygen atom of α-hydroxyacetylene interact to be located 2.324 Å from each other. Reductive heterocoupling at **K** leads to **M**, which resembles **C** and **I**, but contains a coordinated (*E*)-phenylpentenynol. The activation energy of the coupling, 24.7 kcal mol$^{-1}$, is higher than those calculated for the insertion and oxidative addition steps. Therefore, C−C bond formation is the rate-determining step of heterocoupling, as observed experimentally. Intermediate **M** dissociates the catalysis product to close the cycle with a low activation energy of 12.1 kcal mol$^{-1}$.

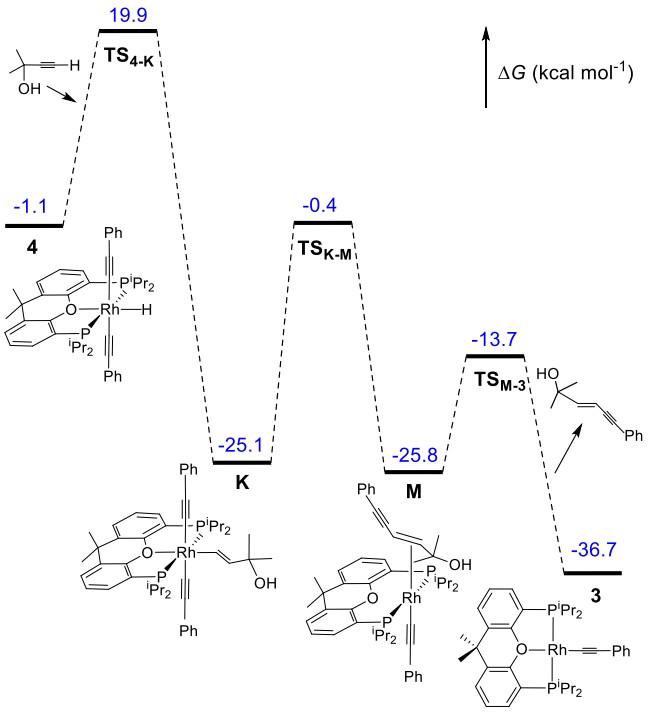


**Figure 6.** Computed energy profile (Δ*G*, in kcal mol$^{-1}$) for the formation of **K**, by insertion of the C−C triple bond of the α-hydroxyacetylene into the R−H bond of **4**, and the release of the heterocoupling product, according to the $C_1$ cycle.

The oxidative additions of the C(sp)−H bond of the alkynes to **3** and **D** that afford the intermediate **J** of the $C_2$ cycle (Figure S114) occur by the same three steps as the oxidative additions schematized in Figure 4. As before, the maximum barriers show values around 21 kcal mol$^{-1}$, which correspond to the sliding of the metal center from the C−C triple bond toward the σ−C−H bond of the added alkyne. Figure 7 shows the energy profile for the formation of **L**, by insertion of the C−C triple bond of α-hydroxyacetylene into the Rh−H bond of **J**, and the release of the heterocoupling product from the latter. The profile for enyne-diol removal by homocoupling is also shown for comparison purposes. The insertion of the C−C triple bond of the α-hydroxyacetylene into the Rh−H bond of **J** has an activation energy of 20.4 kcal mol$^{-1}$. This barrier is similar to the barriers of the functionalized alkyne insertions in the other hydride-rhodium(III) intermediates. The reason is that all insertions have similar transition states. These barriers are also similar to those calculated for oxidative additions of the C(sp)−H bond of alkynes to Rh(I)-acetylide species. However, the reductive C−C bond formation in **L** shows an activation energy of 25.0 kcal mol$^{-1}$, which is higher than the barriers of the oxidative addition and insertion reactions of the cycle. This value is similar to that calculated for the same reductive elimination in **K** but slightly lower than that calculated for the reductive homocoupling in the same intermediate, 26.6 kcal mol$^{-1}$. Therefore, in a consistent manner with the experimental findings, we can say from the DFT calculations: (i) the reductive C−C elimination in **L** is the rate-determining step of the $C_2$ cycle; (ii) the rate-determining step of cycles $C_1$ and $C_2$ is the same; (iii) it also has the same value; and (iv) this value is lower than the activation energy for the C−C reductive elimination of the enyne-diol homocoupling product. The reductive C−C couplings in **L** lead to intermediates **N** and **O**, which dissociate the catalysis products, overcoming low barriers.

**Ethisterone Reactions.** Ethisterone is a good example of a highly functionalized aliphatic α-hydroxyacetylene with a tertiary alcohol character. Its structural modification is of interest, given the important pharmaceutical uses of progestin.[38] It undergoes some organic transformations typical of α-hydroxyacetylenes[39] and has been shown to bind to transition metals, forming metal−carbon bonds.[40] Zhou, Yin, and co-workers reported a Cu-catalyzed dehydrogenative ethisterone-phenylacetylene cross-coupling, giving 1,3-diyne.[41] To demonstrate the remarkable potential of complex **1** as a precursor to homo- and cross-coupling reactions involving α-hydroxyacetylenes, we have also carried out ethisterone homocoupling and ethisterone-phenylacetylene cross-coupling (Scheme 8).

Complex **1** catalyzes the head-to-head dimerization of ethisterone to selectively give the product (*E*)-enyne-diol $\mathbf{a_8}$. This dimer was formed in 56% yield, after 48 h, using 5 mol % of precursor with regard to ethisterone, in benzene, at 80 °C. The cross-coupling reaction was carried out with equimolar concentrations of phenylacetylene and ethisterone, using 10 mol % of complex **1** with respect to each alkyne. In benzene, at 80 °C, the asymmetrical (*E*)-enyn-ol $\mathbf{b_8}$ was formed with a yield of 65%, after 48 h. The products of both reactions were separated from the crude by column chromatography, isolated in 48% and 56% yield, and characterized by $^{1}H$ and $^{13}C\{^{1}H\}$ NMR spectroscopy and high-resolution mass spectrometry.


https://doi.org/10.1021/acscatal.4c00264
ACS Catal. 2024, 14, 8389−8404

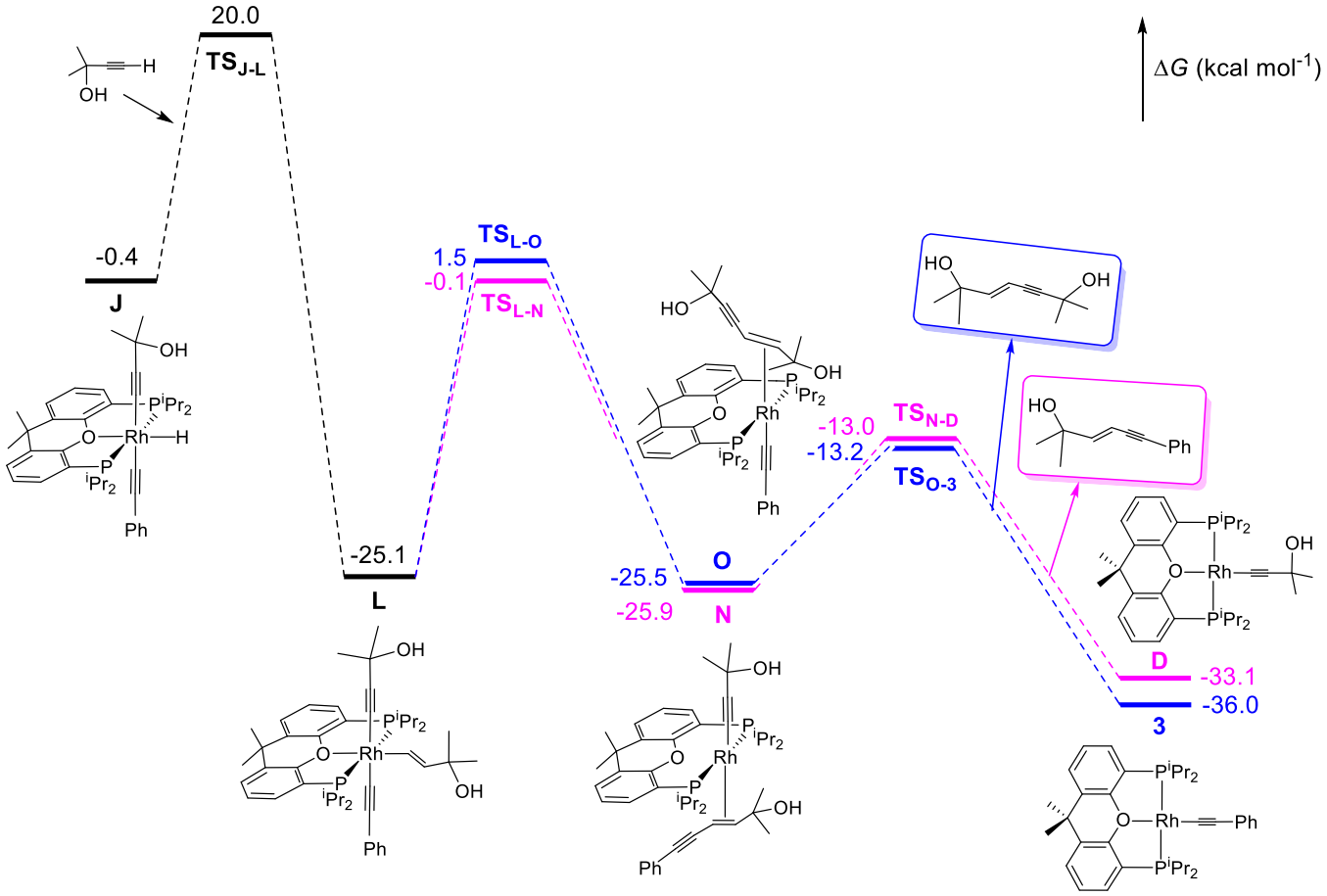


**Figure 7.** Energy profile ($\Delta G$, in kcal mol$^{-1}$) for the formation of **L** and the release of the heterocoupling product (in purple) or the enyne-diol (in blue) from it.

**Scheme 8. Ethisterone Homocoupling and Ethisterone-Phenylacetylene Cross-Coupling**[a]

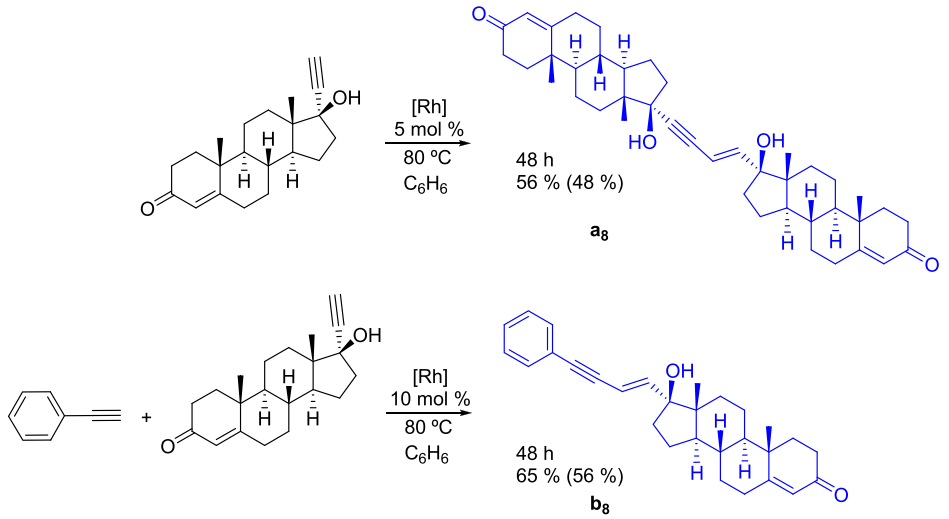


[a]Conditions homocoupling: **1** (5 mg, 0.009 mmol), 0.20 mmol of ethisterone, and benzene (2 mL). Heterocoupling: **1** (5 mg, 0.009 mmol), 0.10 mmol of ethisterone, 0.10 mmol phenylacetylene, and benzene (2 mL). Yields were determined by $^1$H NMR with respect to starting alkyne; isolated yields are given in parentheses.

## CONCLUDING REMARKS

This study has revealed that the square-planar rhodium(I) monohydride complex RhH{$\kappa^3$-*P*,*O*,*P*-[xant(P$^i$Pr$_2$)$_2$]} is an efficient catalyst precursor for the head-to-head homocoupling of terminal alkynes and the head-to-head cross-coupling between phenylacetylenes and $\alpha$-hydroxyacetylenes. Homocoupling reactions give (*E*)-enyne products, while cross-coupling reactions lead to (*E*)-enyn-ols of the type (*E*)-5-phenyl-2-penten-4-yn-1-ol.



https://doi.org/10.1021/acscatal.4c00264
ACS Catal. 2024, 14, 8389−8404

Homocoupling reactions occur as follows: the monohydride complex generates rhodium(I)-acetylide species, which are responsible for catalysis. These square planar derivatives, a different one for each alkyne, oxidatively add the C(sp)-H bond of the substrates to produce bis(acetylide)-rhodium(III)-hydride intermediates, which undergo *anti*-Markovnikov insertion of the C−C triple bond of a new alkyne molecule in the Rh−H bond. The resulting {(*E*)-alkenyl}-rhodium(III)-bis(acetylide) complexes reductively remove the (*E*)-enyne products, regenerating the rhodium(I)-acetylide catalysts. The rate-determining step of the coupling depends on the nature of the alkyne, being the insertion of the C−C triple bond at the Rh−H bond for phenylacetylenes and the reductive elimination of the (*E*)-enyne-diol product for α-hydroxyacetylenes.

Cross-coupling reactions take place through two cycles similar to the cycle that produces homocoupling. They start from the rhodium(I)-acetylide species that generate the two different alkynes involved in each reaction. For both cycles, the rate-determining step is the reductive elimination of the (*E*)-5-phenyl-2-penten-4-yn-1-ol-type products.

The observation of metallic intermediates in organic reactions catalyzed by metals allows for establishing the catalytic cycle and understanding the origin of selectivity. Starting from this premise, we have discovered the mechanism of the homocoupling of phenylacetylenes and α-hydroxyacetylenes, promoted by a highly efficient catalyst precursor, including the rate-determining steps of both dimerizations. DFT calculations reproduce the experimental findings and corroborate the conclusions provided by them. The information obtained in this way has led us to develop cross-coupling reactions between phenylacetylenes and one of the widest ranges of α-hydroxyacetylenes used to date. We can say that there is now a rhodium catalyst precursor for preparing in almost quantitative yield reported and unreported compounds of the type (*E*)-5-phenyl-2-penten-4-yn-1-ol, by direct cross-coupling between phenylacetylenes and α-hydroxyacetylenes.

## EXPERIMENTAL SECTION

**General Information.** All reactions were carried out with the exclusion of air using Schlenk-tube techniques or in a glovebox. Instrumental methods and X-ray details are given in the Supporting Information. In the NMR spectra (Figures S1−S113), the chemical shifts (in ppm) were referenced to residual solvent peaks ($^1$H, $^{13}$C{$^1$H}) or external 85% $H_3PO_4$ ($^{31}$P{$^1$H}), while *J* and *N* ($N = J_{P-H} + J_{P'-H}$ for $^1$H and $N = J_{P-C} + J_{P'-C}$ for $^{13}$C{$^1$H}) were given in hertz. RhH{$\kappa^3$-*P,O,P*-[xant(P$^i$Pr$_2$)$_2$]} (**1**)[30] was prepared according to the reported procedure.

**Spectroscopic Detection of Rh{(*E*)−CH═CHPh}{$\kappa^3$-*P,O,P*-[xant(P$^i$Pr$_2$)$_2$]} (2).** To a NMR tube containing **1** (10 mg, 0.018 mmol), a solution of phenylacetylene in benzene-$d_6$ (0.4 mL, 64 mM; 1.4 equiv) was added. The $^1$H and $^{31}$P{$^1$H} NMR spectra recorded after 5 min at room temperature show the presence of complexes **2**, **3**, and styrene in a 1:0.2:0.2 ratio. Distinctive spectroscopic data for complex **2**: $^1$H NMR (300 MHz, benzene-$d_6$, 298 K): δ 9.90 (ddt, $^3J_{H-H}$ = 17, $^2J_{H-Rh}$ = 3, $^3J_{H-P}$ = 6, Rh−CH═). $^{31}$P{$^1$H} NMR (121.49 MHz, benzene-$d_6$, 298 K): δ 38.6 (d, $^1J_{P-Rh}$ = 176 Hz).

**Preparation of Rh(C≡CPh){$\kappa^3$-*P,O,P*-[xant(P$^i$Pr$_2$)$_2$]} (3).** A solution of **1** (100 mg, 0.18 mmol) in pentane (3 mL) was treated with phenylacetylene (50 μL, 0.46 mmol) and then stirred overnight at room temperature. After that time, it was evaporated to dryness, getting a brown residue. The addition of pentane (4 mL) afforded a white solid that was washed with pentane (2 × 2 mL) and dried in vacuo. Yield: 109 mg (92%). Anal. Calcd for $C_{35}H_{45}OP_2Rh$ (%): C, 65.01; H, 7.01. Found: C, 64.69; H, 7.18. HRMS (electrospray, *m*/*z*): calcd for $C_{35}H_{46}OP_2Rh$ $[M + H]^+$, 647.2073; found, 647.2061. IR ($cm^{-1}$): ν(C≡C) 2088 (m), ν(C−O−C) 1208 (m). $^1$H NMR (300.13 MHz, benzene-$d_6$, 298 K): δ 7.72 (dd, $^3J_{H-H}$ = 8.2, $^4J_{H-H}$ = 1.2, 2H, Ph), 7.28−7.19 (4H, 2H CH-arom POP + 2H Ph), 7.04−6.97 (3H, 2H CH-arom POP + 1H Ph), 6.85 (t, $^3J_{H-H}$ = 7.5, 2H, CH-arom POP), 2.43 (m, 4H, PC*H*(CH$_3$)$_2$), 1.64 (dvt, $^3J_{H-H}$ = 7.2, *N* = 16.5, 12H, PCH(C*H*$_3$)$_2$), 1.20 (s, 6H, CH$_3$), 1.18 (dvt, $^3J_{H-H}$ = 7.2, *N* = 14.8, 12H, PCH(C*H*$_3$)$_2$). $^{13}$C{$^1$H}-apt NMR (75.48 MHz, benzene-$d_6$, 298 K): δ 157.1 (vt, *N* = 16.4, C-arom POP), 132.4 (s, C-arom POP), 131.2 (s, CH-arom POP), 131.1 (m, C Ph), 130.9 (s, CH Ph), 128.2 (s, CH Ph), 127.9 (s, CH-arom POP), 126.0 (vt, *N* = 15.9, C-arom POP), 124.8 (s, CH-arom POP), 123.8 (dt, $^2J_{C-Rh}$ = 20.1, $^3J_{C-P}$ = 4.2, Rh−C≡CPh), 122.9 (s, CH Ph), 110.0 (dt, $^1J_{C-Rh}$ = 62.0, $^2J_{C-P}$ = 19.2, Rh−C≡CPh), 34.1 (s, *C*(CH$_3$)$_2$), 32.5 (s, C(*C*H$_3$)$_2$), 27.2 (dvt, $^3J_{C-Rh}$ = 2.3, N = 10.0, PCH(*C*H$_3$)$_2$), 20.0 (vt, *N* = 8.0, PCH(*C*H$_3$)$_2$), 19.6 (s, PCH(*C*H$_3$)$_2$). $^{31}$P{$^1$H} NMR (121.49 MHz, benzene-$d_6$, 298 K): δ 45.5 (d, $^1J_{Rh-P}$ = 152).

**Reaction of Rh(C≡CPh){$\kappa^3$-*P,O,P*-[xant(P$^i$Pr$_2$)$_2$]} (3) with Phenylacetylene. Spectroscopic Detection of RhH(C≡CPh)$_2${$\kappa^3$-*P,O,P*-[xant(P$^i$Pr$_2$)$_2$]} (4) and Rh{(*E*)−CH═CHPh}(C≡CPh)$_2${$\kappa^3$-*P,O,P*-[xant(P$^i$Pr$_2$)$_2$]} (5).** A NMR tube containing a solution of **3** (15 mg, 0.02 mmol) in benzene-$d_6$ (0.4 mL) was treated with phenylacetylene (25 μL, 0.23 mmol). The $^1$H and $^{31}$P{$^1$H} NMR spectra recorded after 10−20 min at room temperature, show the presence of complexes **3**, **4**, and **5** in an approximate 25:67:8 molar ratio. Distinctive spectroscopic data for complex **4**: $^1$H NMR (300 MHz, benzene-$d_6$, 298 K): δ −18.84 (dt, $^1J_{H-Rh}$ = 32.2, $^2J_{H-P}$ = 12.0, RhH). $^{31}$P{$^1$H} NMR (121.49 MHz, benzene-$d_6$, 298 K): δ 54.4 (d, $^1J_{P-Rh}$ = 100 Hz). Distinctive spectroscopic data for complex **5**: $^1$H NMR (300 MHz, benzene-$d_6$, 298 K): δ 8.58 (ddt, $^3J_{H-H}$ = 14.3, $^3J_{H-P}$ = 2.1, $^2J_{H-Rh}$ = 1.2, Rh−CH═). $^{31}$P{$^1$H} NMR (121.49 MHz, benzene-$d_6$, 298 K): δ 32.9 (d, $^1J_{P-Rh}$ = 100 Hz). Complex **5** was generated as an almost exclusive organometallic species under the following conditions: **3** (15 mg, 0.02 mmol), phenylacetylene (38 μL, 0.35 mmol), benzene-$d_6$ (0.4 mL), 2 h, and room temperature.

**Preparation of Rh{(*E*)−CH═CHC(OH)Ph$_2$}{C≡CC(OH)Ph$_2$}$_2${$\kappa^3$-*P,O,P*-[xant(P$^i$Pr$_2$)$_2$]} (6).** A solution of **1** (100 mg, 0.18 mmol) in benzene (3 mL) was treated with 1,1-diphenyl-2-propyn-1-ol (152 mg, 0.73 mmol) and then stirred at room temperature for 1 h. After that time, the solution was evaporated to dryness, to give a brown residue. The addition of pentane (4 mL) afforded a white solid that was washed with pentane (2 × 2 mL) and dried in vacuo. Yield: 175 mg (82%). Anal. Calcd for $C_{72}H_{75}O_4P_2Rh$ (%): C, 73.96; H, 6.47. Found: C, 73.94; H, 6.50. HRMS (electrospray, *m*/*z*): calcd for $C_{72}H_{75}NaO_4P_2Rh$ $[M + Na]^+$, 1191.4088; found, 1191.4127. IR ($cm^{-1}$): ν(O−H) 3607 (w), ν(C≡C) 2094 (w), ν(C−O−C) 1244 (m), ν(C−O) 1183 and 1150 (m). $^1$H NMR (500.13 MHz, benzene-$d_6$, 298 K): δ 7.78 (d, $^3J_{H-H}$ = 8.4, 4H, Ph) δ 7.52 (d, $^3J_{H-H}$ = 8.4, 8H, Ph), 7.35 (d, $^3J_{H-H}$ = 14.0, 1H, CH═CH), 7.27 (t, $^3J_{H-H}$ = 7.7, 4H, Ph), 7.18−6.92 (19H, 4H CH-arom POP, 1H CH = CH, 14H Ph), 6.86 (t, $^3J_{H-H}$ = 7.8, 2H, CH-arom POP), 2.72 (m, 4H, PC*H*(CH$_3$)$_2$), 2.26 (s, 1H, OH), 2.13 (s, 2H, OH), 1.20 (s, 6H, CH$_3$), 1.07 (dvt, $^3J_{H-H}$ = 7.6, *N* = 12.3, 12H, PCH(C*H*$_3$)$_2$), 1.05


https://doi.org/10.1021/acscatal.4c00264
ACS Catal. 2024, 14, 8389−8404

(dvt, $^3J_{H-H}$ = 7.6, $N$ = 12.3, 12H, PCH($CH_3$)$_2$). $^{13}C\{^1H\}$-apt NMR (75.48 MHz, benzene-$d_6$, 298 K): $\delta$ 156.7 (vt, $N$ = 11.0, $C$-arom POP), 148.9, 148.6 (s, C Ph), 139.0 (t, $^3J_{C-P}$ = 3.7, Rh−CH═CH), 133.5 (vt, $N$ = 5.1, C-arom POP), 130.2 (s, CH-arom POP), 129.7 (dt, $^1J_{C-Rh}$ = 34.1, $^2J_{C-P}$ = 9.9, Rh−CH═CH), 128.0, 127.8, 127.8 (s, CH Ph), 127.1, 126.7, 126.4 (s, CH-arom POP), 124.6 (vt, $N$ = 5.3, CH-arom POP), 123.3 (vt, $N$ = 14.2, C-arom POP), 113.4 (dt, $^1J_{C-Rh}$ = 38.9, $^2J_{C-P}$ = 15.5, Rh−$C$≡CC(OH)Ph$_2$), 109.8 (dt, $^2J_{C-Rh}$ = 3.0, $^3J_{C-P}$ = 0.8, Rh−C≡$C$C(OH)Ph$_2$), 80.4 (dt, $^3J_{C-Rh}$ = 3.0, $^4J_{C-P}$ = 0.8, $C$(OH)Ph$_2$), 75.5 (s, $C$(OH)Ph$_2$), 35.0 (s, C($CH_3$)$_2$), 29.0 (s, $C$(CH$_3$)$_3$), 25.8 (vt, $N$ = 24.9, PCH($CH_3$)$_2$), 19.0, 18.9 (both s, PCH($CH_3$)$_2$). $^{31}P\{^1H\}$ NMR (202.46 MHz, benzene-$d_6$, 298 K): $\delta$ 34.6 (d, $^1J_{Rh-P}$ = 101.5).

**Kinetic Analysis of the Reductive Elimination of (*E*)-1,1,6,6-Tetraphenyl-2-hexen-4-yne-1,6-diol from Rh{(*E*)−CH═CHC(OH)Ph$_2$}{C≡CC(OH)Ph$_2$}{$\kappa^3$-*P,O,P*-[xant-(P$^i$Pr$_2$)$_2$]} (6).** The experimental procedure is described for a particular case, but the same method was used in all experiments. In the glovebox, a NMR tube was charged with a solution of **6** (10 mg, 0.008 mmol) in benzene-$d_6$ (0.4 mL), and a sealed capillary tube filled with a solution of the internal standard ($PPh_3$) in benzene-$d_6$ was placed in the NMR tube. The tube was immediately introduced into a NMR probe preheated at the desired temperature (353, 343, 333, and 323 K), and the reaction was monitored by $^{31}P\{^1H\}$ NMR at different intervals of time. With these experiments and using eq 1 the rate constants $k$ were calculated

$$\ln\frac{[\mathbf{6}]}{[\mathbf{6}]_0} = -kt \tag{1}$$

**Kinetic Analysis of the Dimerization of 1,1-Diphenyl-2-propyn-1-ol Catalyzed by Rh{(*E*)−CH═CHC(OH)Ph$_2$}-{C≡CC(OH)Ph$_2$}$_2${$\kappa^3$-*P,O,P*-[xant(P$^i$Pr$_2$)$_2$]} (6).** The experimental procedure is described for a particular case, but the same method was used in all experiments. In the glovebox, a screw-cap NMR tube was charged with **6** (10 mg, 0.008 mmol), 1,1-diphenyl-2-propyn-1-ol (71 mg, 0.34 mmol), and a sealed capillary tube filled with a solution of the internal standard (dioxane) in benzene-$d_6$ was placed in the NMR tube. In the NMR room, 0.4 mL of benzene-$d_6$ was added to that tube through the septum of the screw-cap, the tube was immediately introduced into a NMR probe preheated at the desired temperature (353, 343, 333, and 323 K), and the reaction was monitored by $^1H$ NMR at different intervals of time. With these experiments and using eq 2 the rate constants $k$ were calculated

$$\frac{1}{[\text{alkyne}]_t} = \frac{1}{[\text{alkyne}]_0} + 2k_{obs}t \tag{2}$$

where

$$k_{obs} = k[\text{catalyst}]$$

**General Procedure for Homocoupling Reactions.** All experiments were performed in duplicate, monitored by $^1H$ NMR spectroscopy, and prepared in a glovebox. The procedure used in all cases was as follows: a NMR tube was loaded with a solution of **1** (5 mg, 0.009 mmol) in benzene-$d_6$ (0.4 mL). Subsequently, a sealed capillary tube containing a solution of the internal standard (dioxane or 1,1,2,2-tetrachloroethane) in benzene-$d_6$ was introduced, and the corresponding alkyne (0.38 mmol) was added. The tube was then closed with a cap, removed from the glovebox, and placed in a thermostatic bath at 80 °C. After completion of the reaction, the solvent was removed, and diethyl ether (phenylacetylenes) or ethyl acetate (alkynols) was added to the crude product. The solution was passed through a silica pad and dried under a vacuum. The products were characterized by $^1H$ and $^{13}C\{^1H\}$ NMR spectroscopies and, in addition, those nonreported by HR-MS.

**General Procedure for the Cross-Coupling Reactions.** The experimental procedure was similar to that described for the homocoupling reactions, but using 0.19 mmol of each alkyne. After completion of the reaction, the crude products were purified by preparative thin layer chromatography eluting with pentane/ethyl acetate 9:1 (2:1 for $\mathbf{e}_6$ and $\mathbf{f}_6$). The products were characterized by $^1H$ and $^{13}C\{^1H\}$ NMR spectroscopies and, in addition, those nonreported by HR-MS.

**Homocoupling of Ethisterone.** Inside the glovebox, ethisterone (63 mg, 0.20 mmol) was added to a solution of **1** (5 mg, 0.009 mmol) in benzene (2 mL) and placed in an Ace pressure tube. The tube was taken out of the glovebox and heated at 80 °C for 48 h. After this time, the solvent was evaporated under reduced pressure to afford a crude reaction mixture, which was dissolved in a minimal amount of ethyl acetate and purified by column chromatography on silica eluting with ethyl acetate/hexane (1:9 to 9:1). The product ($\mathbf{a}_8$) was characterized by $^1H$ and $^{13}C\{^1H\}$ NMR spectroscopies and by HR-MS.

**Cross-Coupling of Ethisterone.** Inside the glovebox, ethisterone (34 mg, 0.11 mmol) and phenylacetylene (12, $\mu$L, 0.11 mmol) were added to a stirred solution of **1** (5 mg, 0.009 mmol) in benzene (2 mL) and placed in an Ace pressure tube. The tube was taken out of the glovebox and heated at 80 °C for 48 h. After this time, the solvent was evaporated under reduced pressure to afford a crude reaction mixture, which was dissolved in a minimal amount of ethyl acetate and purified by column chromatography on silica eluting with ethyl acetate/hexane (1:9 to 9:1). The product ($\mathbf{b}_8$) was characterized by $^1H$ and $^{13}C\{^1H\}$ NMR spectroscopies and by HR-MS.

## ■ ASSOCIATED CONTENT

### Supporting Information

The Supporting Information is available free of charge at https://pubs.acs.org/doi/10.1021/acscatal.4c00264.

General information for the Experimental Section, characterization data of the coupling products, structural analysis, computational details, and NMR spectra (PDF)
Cartesian coordinates of calculated structures (XYZ)
CIF file of complex **6** (CIF)

### Accession Codes

CCDC 2283937 contains the supplementary crystallographic data for this paper. These data can be obtained free of charge via www.ccdc.cam.ac.uk/data_request/cif, or by emailing data_request@ccdc.cam.ac.uk, or by contacting The Cambridge Crystallographic Data Centre, 12 Union Road, Cambridge CB2 1EZ, UK; fax: +44 1223 336033)

## ■ AUTHOR INFORMATION

### Corresponding Author

**Miguel A. Esteruelas** − *Departamento de Química Inorgánica—Instituto de Síntesis Química y Catálisis Homogénea (ISQCH)—Centro de Innovación en Química Avanzada (ORFEO-CINQA), Universidad de Zaragoza—CSIC, 50009 Zaragoza, Spain;* orcid.org/0000-0002-4829-7590; Email: maester@unizar.es



https://doi.org/10.1021/acscatal.4c00264
*ACS Catal.* 2024, 14, 8389−8404

## Authors

**Laura A. de las Heras** − *Departamento de Química Inorgánica—Instituto de Síntesis Química y Catálisis Homogénea (ISQCH)—Centro de Innovación en Química Avanzada (ORFEO-CINQA), Universidad de Zaragoza—CSIC, 50009 Zaragoza, Spain*

**Montserrat Oliván** − *Departamento de Química Inorgánica—Instituto de Síntesis Química y Catálisis Homogénea (ISQCH)—Centro de Innovación en Química Avanzada (ORFEO-CINQA), Universidad de Zaragoza—CSIC, 50009 Zaragoza, Spain;* orcid.org/0000-0003-0381-0917

**Enrique Oñate** − *Departamento de Química Inorgánica—Instituto de Síntesis Química y Catálisis Homogénea (ISQCH)—Centro de Innovación en Química Avanzada (ORFEO-CINQA), Universidad de Zaragoza—CSIC, 50009 Zaragoza, Spain;* orcid.org/0000-0003-2094-719X

Complete contact information is available at: https://pubs.acs.org/10.1021/acscatal.4c00264


## Notes

The authors declare no competing financial interest.

## ■ ACKNOWLEDGMENTS

Financial support from the MICIN/AEI/10.13039/501100011033 (PID2020-115286GB-I00 and RED2022-134287-T), Gobierno de Aragón (E06_23R and LMP23_21), FEDER, and the European Social Fund is acknowledged. L.A.d.l.H. thanks the MECD for her FPU contract (FPU17/04813, "ESF investing in your future").

## ■ REFERENCES


(1) (a) Bao, X.; Ren, J.; Yang, Y.; Ye, X.; Wang, B.; Wang, H. 2-Activated 1,3-enynes in enantioselective synthesis. *Org. Biomol. Chem.* **2020**, *18*, 7977−7986. (b) Fu, L.; Greßies, S.; Chen, P.; Liu, G. Recent Advances and Perspectives in Transition Metal-Catalyzed 1,4-Functionalizations of Unactivated 1,3-Enynes for the Synthesis of Allenes. *Chin. J. Chem.* **2020**, *38*, 91−100. (c) Liu, Y.; Luo, P.; Fu, Y.; Hao, T.; Liu, X.; Ding, Q.; Peng, Y. Recent advances in the tandem annulation of 1,3-enynes to functionalized pyridine and pyrrole derivatives. *Beilstein J. Org. Chem.* **2021**, *17*, 2462−2476.

(2) (a) Garcia-Garrido, S. E. Catalytic Dimerization of Alkynes. In *Modern Alkyne Chemistry*; Trost, B. M., Li, C.-J., Eds.; Wiley: Weinheim, Germany, 2015; pp 301−334. (b) Trost, B. M.; Masters, J. T. Transition metal-catalyzed couplings of alkynes to 1,3-enynes: modern methods and synthetic applications. *Chem. Soc. Rev.* **2016**, *45*, 2212−2238. (c) Temkin, O. N. Golden Age" of Homogeneous Catalysis Chemistry of Alkynes: Dimerization and Oligomerization of Alkynes. *Kinet. Catal.* **2019**, *60*, 689−732. (d) Babón, J. C.; Esteruelas, M. A.; López, A. M. Homogeneous catalysis with polyhydride complexes. *Chem. Soc. Rev.* **2022**, *51*, 9717−9758.

(3) Esteruelas, M. A.; Herrero, J.; López, A. M.; Oliván, M. Alkyne-Coupling Reactions Catalyzed by $OsHCl(CO)(P^iPr_3)_2$ in the Presence of Diethylamine. *Organometallics* **2001**, *20*, 3202−3205.

(4) (a) Lee, C.-C.; Lin, Y.-C.; Liu, Y.-H.; Wang, Y. Rhodium-Catalyzed Dimerization of Terminal Alkynes Assisted by MeI. *Organometallics* **2005**, *24*, 136−143. (b) Gorgas, N.; Alves, L. G.; Stöger, B.; Martins, A. M.; Veiros, L. F.; Kirchner, K. Stable, Yet Highly Reactive Nonclassical Iron(II) Polyhydride Pincer Complexes: *Z*-Selective Dimerization and Hydroboration of Terminal Alkynes. *J. Am. Chem. Soc.* **2017**, *139*, 8130−8133. (c) Gorgas, N.; Stöger, B.; Veiros, L. F.; Kirchner, K. Iron(II) Bis(acetylide) Complexes as Key Intermediates in the Catalytic Hydrofunctionalization of Terminal Alkynes. *ACS Catal.* **2018**, *8*, 7973−7982. (d) Storey, C. M.; Gyton, M. R.; Andrew, R. E.; Chaplin, A. B. Terminal Alkyne Coupling Reactions through a Ring: Mechanistic Insights and Regiochemical Switching. *Angew. Chem., Int. Ed.* **2018**, *57*, 12003−12006. (e) Liang, Q.; Sheng, K.; Salmon, A.; Zhou, V. Y.; Song, D. Active Iron(II) Catalysts toward gem-Specific Dimerization of Terminal Alkynes. *ACS Catal.* **2019**, *9*, 810−818. (f) Zhuang, X.; Chen, J.-Y.; Yang, Z.; Jia, M.; Wu, C.; Liao, R.-Z.; Tung, C.-H.; Wang, W. Sequential Transformation of Terminal Alkynes to 1,3-Dienes by a Cooperative Cobalt Pyridonate Catalyst. *Organometallics* **2019**, *38*, 3752−3759. (g) Galiana-Cameo, M.; Borraz, M.; Zelenkova, Y.; Passarelli, V.; Lahoz, F. J.; Pérez-Torrente, J. J.; Oro, L. A.; Di Giuseppe, A.; Castarlenas, R. Rhodium(I)-NHC Complexes Bearing Bidentate Bis-Heteroatomic Acidato Ligands as *gem*-Selective Catalysts for Alkyne Dimerization. *Chem.—Eur. J.* **2020**, *26*, 9598−9608. (h) Storey, C. M.; Gyton, M. R.; Andrew, R. E.; Chaplin, A. B. Terminal Alkyne Coupling Reactions Through a Ring: Effect of Ring Size on Rate and Regioselectivity. *Chem.—Eur. J.* **2020**, *26*, 14715−14723. (i) Pfeffer, C.; Wannenmacher, N.; Frey, W.; Peters, R. Stereo- and Regioselective Dimerization of Alkynes to Enynes by Bimetallic Syn-Carbopalladation. *ACS Catal.* **2021**, *11*, 5496−5505. (j) Thompson, C. V.; Narro, A. L.; Arman, H. D.; Tonzetich, Z. J. Synthesis and Reactivity of Iron(II) Acetylide Complexes Relevant to Alkyne Dimerization. *Organometallics* **2022**, *41*, 2291−2300.

(5) (a) Kovalev, I. P.; Yevdakov, K. V.; Strelenko, Y. A.; Vinogradov, M. G.; Nikishin, G. I. Dimerization of 1-alkynes catalyzed by $RhCl(PMe_3)_3$. Isolation of the intermediate (alkynyl)(vinyl)rhodium-(III) complexes. *J. Organomet. Chem.* **1990**, *386*, 139−146. (b) Geer, A. M.; Julián, A.; López, J. A.; Ciriano, M. A.; Tejel, C. Pseudo-tetrahedral Rhodium and Iridium Complexes: Catalytic Synthesis of *E*-Enynes. *Chem.—Eur. J.* **2018**, *24*, 17545−17556.

(6) Vardanyan, R. S.; Hruby, V. J. Female Sex Hormones. In *Synthesis of Essential Drugs*; Elsevier, 2006; Chapter 28, pp 365−379..

(7) (a) Stanczyk, F. Z. Pharmacokinetics and Potency of Progestins used for Hormone Replacement Therapy and Contraception. *Rev. Endocr. Metab. Disord.* **2002**, *3* (3), 211−224. (b) Sonneveld, E.; Pieterse, B.; Schoonen, W. G.; van der Burg, B. Validation of *in vitro* screening models for progestagenic activities: Inter-assay comparison and correlation with *in vivo* activity in rabbits. *Toxicol. In Vitro* **2011**, *25*, 545−554. (c) Bhatti, H. N.; Khera, R. A. Biological transformations of steroidal compounds: A review. *Steroids* **2012**, *77*, 1267−1290.

(8) Alonso, F.; Beletskaya, I. P.; Yus, M. Transition-Metal-Catalyzed Addition of Heteroatom-Hydrogen Bonds to Alkynes. *Chem. Rev.* **2004**, *104*, 3079−3160.

(9) (a) Singer, H.; Wilkinson, G. The Dimerisation of Monosubstituted α-Hydroxyacetylenes by Use of Tris(triphenylphosphine)-chlororhodium(I) as Catalyst. *J. Chem. Soc. A* **1968**, *0*, 849−853. (b) Schmitt, H. J.; Singer, H. Die dimerisierung von endständigen α-hydroxyacetylenen mit rhodiumkomplexkatalysatoren. *J. Organomet. Chem.* **1978**, *153*, 165−179. (c) Schäfer, H.-A.; Marcy, R.; Rüping, T.; Singer, H. Die oligomerisierung endständiger hydroxyacetylene mit rhodiumkomplexkatalysatoren. *J. Organomet. Chem.* **1982**, *240* (1), 17−25. (d) Weng, W.; Guo, C.; Çelenligil-Çetin, R.; Foxman, B. M.; Ozerov, O. V. Skeletal change in the PNP pincer ligand leads to a highly regioselective alkyne dimerization catalyst. *Chem. Commun.* **2006**, 197−199. (e) Richard, M. E.; Reese, K. P.; Stone, J. J.; Pickett, P. D.; Tillman, E. S.; Stockland, R. A., Jr. Probing the steric limits of rhodium catalyzed hydrophosphinylation. P-H addition vs. dimerization/oligomerization/polymerization. *J. Organomet. Chem.* **2011**, *696*, 123−129.

(10) (a) Sabourin, E. T. the selective head-to-tail dimerization of α-hydroxy terminal acetylenes. *J. Mol. Catal.* **1984**, *26*, 363−373. (b) Trost, B. M.; Chan, C.; Ruhter, G. Metal-Mediated Approach to Enynes. *J. Am. Chem. Soc.* **1987**, *109*, 3486−3487.

(11) Babón, J. C.; Esteruelas, M. A.; Oñate, E.; Paz, S.; Vélez, A. Silyl-Osmium(IV)-Trihydride Complexes Stabilized by a Pincer Ether-Diphosphine: Formation and Reactions with Alkynes. *Organometallics* **2022**, *41*, 2022−2034.

(12) Oshovsky, G. V.; Hessen, B.; Reek, J. N. H.; De Bruin, B. Electronic Selectivity Tuning in Titanium(III)-Catalyzed Acetylene Cross-Dimerization Reactions. *Organometallics* **2011**, *30*, 6067−6070.

(13) (a) Katayama, H.; Yari, H.; Tanaka, M.; Ozawa, F. (*Z*)-Selective cross-dimerization of arylacetylenes with silylacetylenes catalyzed by vinylideneruthenium complexes. *Chem. Commun.* **2005**, 4336−4338. (b) Weber, S.; Veiros, L. F.; Kirchner, K. Selective Manganese-Catalyzed Dimerization and Cross-Coupling of Terminal Alkynes. *ACS Catal.* **2021**, *11* (11), 6474−6483.

(14) (a) Trost, B. M.; Matsubara, S.; Caringi, J. J. Cycloisomerization of $\alpha,\omega$-Diynes to Macrocycles. *J. Am. Chem. Soc.* **1989**, *111*, 8745−8746. (b) Xu, H.-D.; Zhang, R.-W.; Li, X.; Huang, S.; Tang, W.; Hu, W.-H. Rhodium-Catalyzed Chemo- and Regioselective Cross-Dimerization of Two Terminal Alkynes. *Org. Lett.* **2013**, *15*, 840−843. (c) Liang, Q.; Osten, K. M.; Song, D. Iron-Catalyzed *gem*-Specific Dimerization of Terminal Alkynes. *Angew. Chem., Int. Ed.* **2017**, *56*, 6317−6320. (d) Liang, Q.; Hayashi, K.; Song, D. Catalytic Alkyne Dimerization without Noble Metals. *ACS Catal.* **2020**, *10*, 4895−4905. (e) Chen, J.-F.; Li, C. Cobalt-Catalyzed gem-Cross-Dimerization of Terminal Alkynes. *ACS Catal.* **2020**, *10*, 3881−3889. (f) Liu, L.; Dong, J.; Fu, Z.; Su, L.; Wu, S.; Shang, Q.; Yin, S.-F.; Zhou, Y. Specific cross-dimerization of terminal alkynes *via* Pd/TMEDA Catalysis. *Sci. China Chem.* **2022**, *65*, 2487−2493.

(15) (a) Trost, B. M.; McIntosh, M. C. An Unusual Selectivity in Pd Catalyzed Cross-Coupling of Terminal Alkynes with "Unactivated" Alkynes. *Tetrahedron Lett.* **1997**, *38*, 3207−3210. (b) Katagiri, T.; Tsurugi, H.; Satoh, T.; Miura, M. Rhodium-catalyzed (*E*)-selective cross-dimerization of terminal alkynes. *Chem. Commun.* **2008**, 3405−3407.

(16) Lauer, M. G.; Headford, B. R.; Gobble, O. M.; Weyhaupt, M. B.; Gerlach, D. L.; Zeller, M.; Shaughnessy, K. H. A Trialkylphosphine-Derived Palladacycle as a Catalyst in the Selective Cross-Dimerization of Terminal Arylacetylenes with Terminal Propargyl Alcohols and Amides. *ACS Catal.* **2016**, *6*, 5834−5842.

(17) Deussen, H.-J.; Jeppesen, L.; Schärer, N.; Junager, F.; Bentzen, B.; Weber, B.; Weil, V.; Mozer, S. J.; Sauerberg, P. Process Development and Scale-Up of the PPAR Agonist NNC 61−4655. *Org. Process Res. Dev.* **2004**, *8*, 363−371.

(18) (a) Kumar, A.; Bhatti, T. M.; Goldman, A. S. Dehydrogenation of Alkanes and Aliphatic Groups by Pincer-Ligated Metal Complexes. *Chem. Rev.* **2017**, *117*, 12357−12384. (b) Gorgas, N.; Kirchner, K. Isoelectronic Manganese and Iron Hydrogenation/Dehydrogenation Catalysts: Similarities and Divergences. *Acc. Chem. Res.* **2018**, *51*, 1558−1569. (c) Shi, R.; Zhang, Z.; Hu, X. Nickamine and Analogous Nickel Pincer Catalysts for Cross-Coupling of Alkyl Halides and Hydrosilylation of Alkenes. *Acc. Chem. Res.* **2019**, *52*, 1471−1483. (d) Alig, L.; Fritz, M.; Schneider, S. First-Row Transition Metal (De)Hydrogenation Catalysis Based On Functional Pincer Ligands. *Chem. Rev.* **2019**, *119*, 2681−2751. (e) González-Sebastián, L.; Morales-Morales, D. Cross-coupling reactions catalysed by palladium pincer complexes. A review of recent advances. *J. Organomet. Chem.* **2019**, *893*, 39−51. (f) Arora, V.; Narjinari, H.; Nandi, P. G.; Kumar, A. Recent advances in pincer-nickel catalyzed reactions. *Dalton Trans.* **2021**, *50*, 3394−3428. (g) Kar, S.; Milstein, D. Sustainable catalysis with fluxional acridine-based PNP pincer complexes. *Chem. Commun.* **2022**, *58*, 3731−3746.

(19) Asensio, G.; Cuenca, A. B.; Esteruelas, M. A.; Medio-Simón, M.; Oliván, M.; Valencia, M. Osmium(III) Complexes with POP Pincer Ligands: Preparation from Commercially Available $OsCl_3{\cdot}3H_2O$ and Their X-ray Structures. *Inorg. Chem.* **2010**, *49*, 8665−8667.

(20) (a) Adams, G. M.; Weller, A. S. POP-type ligands: Variable coordination and hemilabile behaviour. *Coord. Chem. Rev.* **2018**, *355*, 150−172. (b) Adams, G. M.; Ryan, D. E.; Beattie, N. A.; McKay, A. I.; Lloyd-Jones, G. C.; Weller, A. S. Dehydropolymerization of $H_3B{\cdot}NMeH_2$ Using a $[Rh(DPEphos)]^+$ Catalyst: The Promoting Effect of $NMeH_2$. *ACS Catal.* **2019**, *9*, 3657−3666.

(21) (a) Esteruelas, M. A.; Oliván, M.; Vélez, A. Xantphos-Type Complexes of Group 9: Rhodium versus Iridium. *Inorg. Chem.* **2013**, *52*, 5339−5349. (b) Alós, J.; Esteruelas, M. A.; Oliván, M.; Oñate, E.; Puylaert, P. C-H Bond Activation Reactions in Ketones and Aldehydes Promoted by POP-Pincer Osmium and Ruthenium Complexes. *Organometallics* **2015**, *34*, 4908−4921. (c) Esteruelas, M. A.; Fernández, I.; García-Yebra, C.; Martín, J.; Oñate, E. Elongated $\sigma$-Borane versus $\sigma$-Borane in Pincer-POP-Osmium Complexes. *Organometallics* **2017**, *36*, 2298−2307. (d) Curto, S. G.; Esteruelas, M. A.; Oliván, M.; Oñate, E.; Vélez, A. Selective C-Cl Bond Oxidative Addition of Chloroarenes to a POP-Rhodium Complex. *Organometallics* **2017**, *36*, 114−128. (e) Esteruelas, M. A.; Fernández, I.; Martínez, A.; Oliván, M.; Oñate, E.; Vélez, A. Iridium-Promoted B-B Bond Activation: Preparation and X-ray Diffraction Analysis of a *mer*-Tris(boryl) Complex. *Inorg. Chem.* **2019**, *58*, 4712−4717. (f) Esteruelas, M. A.; Fernández, I.; García-Yebra, C.; Martín, J.; Oñate, E. Cycloosmathioborane Compounds: Other Manifestations of the Hückel Aromaticity. *Inorg. Chem.* **2019**, *58*, 2265−2269. (g) de las Heras, L. A.; Esteruelas, M. A.; Oliván, M.; Oñate, E. Rhodium-Promoted C−H Bond Activation of Quinoline, Methylquinolines, and Related Mono-Substituted Quinolines. *Organometallics* **2022**, *41*, 2317−2326.

(22) Esteruelas, M. A.; Oliván, M. Osmium Complexes with POP Pincer Ligands. In *Pincer Compounds: Chemistry and Applications*; Morales-Morales, D., Ed.; Elsevier, 2018; Chapter 16, pp 341−357..

(23) Antiñolo, A.; Esteruelas, M. A.; García-Yebra, C.; Martín, J.; Oñate, E.; Ramos, A. Reactions of an Osmium(IV)-Hydroxo Complex with Amino-Boranes: Formation of Boroxide Derivatives. *Organometallics* **2019**, *38*, 310−318.

(24) (a) Esteruelas, M. A.; García-Yebra, C.; Martín, J.; Oñate, E. *mer*, *fac*, and Bidentate Coordination of an Alkyl-POP Ligand in the Chemistry of Nonclassical Osmium Hydrides. *Inorg. Chem.* **2017**, *56*, 676−683. (b) Curto, S. G.; de las Heras, L. A.; Esteruelas, M. A.; Oliván, M.; Oñate, E.; Vélez, A. Reactions of POP-pincer rhodium(I)-aryl complexes with small molecules: coordination flexibility of the ether diphosphine. *Can. J. Chem.* **2021**, *99*, 127−136. (c) Esteruelas, M. A.; Oñate, E.; Paz, S.; Vélez, A. Repercussion of a 1,3-Hydrogen Shift in a Hydride-Osmium-Allenylidene Complex. *Organometallics* **2021**, *40*, 1523−1537.

(25) Alós, J.; Bolaño, T.; Esteruelas, M. A.; Oliván, M.; Oñate, E.; Valencia, M. POP-Pincer Ruthenium Complexes: $d^6$ Counterparts of Osmium $d^4$ Species. *Inorg. Chem.* **2014**, *53*, 1195−1209.

(26) (a) Alós, J.; Bolaño, T.; Esteruelas, M. A.; Oliván, M.; Oñate, E.; Valencia, M. POP-Pincer Osmium-Polyhydrides: Head-to-Head (*Z*)-Dimerization of Terminal Alkynes. *Inorg. Chem.* **2013**, *52*, 6199−6213. (b) Esteruelas, M. A.; García-Yebra, C.; Martín, J.; Oñate, E. Dehydrogenation of Formic Acid Promoted by a Trihydride-Hydroxo-Osmium(IV) Complex: Kinetics and Mechanism. *ACS Catal.* **2018**, *8*, 11314−11323.

(27) (a) Esteruelas, M. A.; Oliván, M.; Vélez, A. Conclusive Evidence on the Mechanism of the Rhodium-Mediated Decyanative Borylation. *J. Am. Chem. Soc.* **2015**, *137*, 12321−12329. (b) Curto, S. G.; Esteruelas, M. A.; Oliván, M.; Oñate, E.; Vélez, A. $\beta$-Borylalkenyl *Z*-*E* Isomerization in Rhodium-Mediated Diboration of Nonfunctionalized Internal Alkynes. *Organometallics* **2018**, *37*, 1970−1978. (c) Curto, S. G.; de las Heras, L. A.; Esteruelas, M. A.; Oliván, M.; Oñate, E. C($sp^3$)-Cl Bond Activation Promoted by a POP-Pincer Rhodium(I) Complex. *Organometallics* **2019**, *38*, 3074−3083. (d) Curto, S. G.; Esteruelas, M. A.; Oliván, M.; Oñate, E. Rhodium-Mediated Dehydrogenative Borylation-Hydroborylation of Bis(alkyl)alkynes: Intermediates and Mechanism. *Organometallics* **2019**, *38*, 2062−2074. (e) Curto, S. G.; Esteruelas, M. A.; Oliván, M.; Oñate, E. Insertion of Diphenylacetylene into Rh−Hydride and Rh−Boryl Bonds: Influence of the Boryl on the Behavior of the $\beta$-Borylalkenyl Ligand. *Organometallics* **2019**, *38*, 4183−4192. (f) de las Heras, L. A.; Esteruelas, M. A.; Oliván, M.; Oñate, E. C-Cl Oxidative Addition and C-C Reductive Elimination Reactions in the Context of the Rhodium-Promoted Direct Arylation. *Organometallics* **2022**, *41*, 716−732.

(28) (a) Esteruelas, M. A.; Oliván, M.; Vélez, A. POP-Pincer Silyl Complexes of Group 9: Rhodium versus Iridium. *Inorg. Chem.* **2013**, *52*, 12108−12119. (b) Esteruelas, M. A.; Martínez, A.; Oliván, M.; Oñate, E. Direct C-H Borylation of Arenes Catalyzed by Saturated Hydride-Boryl-Iridium-POP Complexes: Kinetic Analysis of the Elemental Steps. *Chem.—Eur. J.* **2020**, *26*, 12632−12644. (c) Esteruelas, M. A.; Martínez, A.; Oliván, M.; Oñate, E. Kinetic Analysis and Sequencing of



https://doi.org/10.1021/acscatal.4c00264
*ACS Catal.* 2024, 14, 8389−8404

Si-H and C-H Bond Activation Reactions: Direct Silylation of Arenes Catalyzed by an Iridium-Polyhydride. *J. Am. Chem. Soc.* **2020**, *142*, 19119−19131.
(29) Esteruelas, M. A.; Oliván, M.; Vélez, A. POP-Rhodium-Promoted C-H and B-H Bond Activation and C-B Bond Formation. *Organometallics* **2015**, *34*, 1911−1924.
(30) Esteruelas, M. A.; Martínez, A.; Oliván, M.; Vélez, A. A General Rhodium Catalyst for the Deuteration of Boranes and Hydrides of the Group 14 Elements. *J. Org. Chem.* **2020**, *85*, 15693−15698.
(31) Esteruelas, M. A.; Nolis, P.; Oliván, M.; Oñate, E.; Vallribera, A.; Vélez, A. Ammonia Borane Dehydrogenation Promoted by a Pincer-Square-Planar Rhodium(I) Monohydride: A Stepwise Hydrogen Transfer from the Substrate to the Catalyst. *Inorg. Chem.* **2016**, *55*, 7176−7181.
(32) Adams, G. M.; Colebatch, A. L.; Skornia, J. T.; McKay, A. I.; Johnson, H. C.; Lloyd−Jones, G. C.; Macgregor, S. A.; Beattie, N. A.; Weller, A. S. Dehydropolymerization of $H_3B{\cdot}NMeH_2$ To Form Polyaminoboranes Using [Rh(Xantphos-alkyl)] Catalysts. *J. Am. Chem. Soc.* **2018**, *140*, 1481−1495.
(33) Barrio, P.; Esteruelas, M. A.; Lledós, A.; Oñate, E.; Tomàs, J. Influence of the Cis Ligand on the H-H Separation and the Rotation Barrier of the Dihydrogen in Osmium-Elongated Dihydrogen Complexes Containing an Ortho-Metalated Ketone. *Organometallics* **2004**, *23*, 3008−3015.
(34) Li, S.-Y.; Zhang, X.; Teng, F.; Li, Y.; Li, J.-H. Rh(III)-Catalyzed [3 + 2]/[4 + 2] annulation of acetophenone oxime ethers with 3-acetoxy-1,4-enynes involving C-H activation. *Org. Chem. Front.* **2021**, *8*, 2955−2962.
(35) (a) Schreurs, P. H. M.; Galesloot, W. G.; Brandsma, L. Base-catalysed cyclisation of *trans*-enyne alcohols to derivatives of furan. *Recl. Trav. Chim. Pays-Bas* **1975**, *94*, 70−72. (b) Li, P.-F.; Wang, H.-L.; Qu, J. 1,*n*-Rearrangement of Allylic Alcohols Promoted by Hot Water: Application to the Synthesis of Navenone B, a Polyene Natural Product. *J. Org. Chem.* **2014**, *79*, 3955−3962.
(36) Li, C.; Lu, W.; Lu, B.; Li, W.; Xie, X.; Zhang, Z. Ru-Catalyzed Chemo- and Enantioselective Hydrogenation of 2,4-Pentadien-1-ones: Synthesis of Chiral 2,4-Pentadien-1-ols. *J. Org. Chem.* **2019**, *84*, 16086−16094.
(37) The lowest field resonance in the spectrum of Figure S14, corresponding to the reaction between phenylacetylene and 1,1-diphenyl-2-propyn-1-ol, is due to **6**.
(38) Forinash, A. B.; Evans, S. L. New Hormonal Contraceptives: A Comprehensive Review of the Literature. *Pharmacotherapy* **2003**, *23*, 1573−1591.
(39) See for example: (a) Hofmeister, H.; Annen, K.; Laurent, H.; Wiechert, R. A Novel Entry to 17$\alpha$-Bromo- and 17$\alpha$-Iodoethynyl Steroids. *Angew. Chem., Int. Ed. Engl.* **1984**, *23*, 727−729. (b) Kumar, D.; Mishra, K. B.; Mishra, B. B.; Mondal, S.; Tiwari, V. K. Click chemistry inspired highly facile synthesis of triazolyl ethisterone glycoconjugates. *Steroids* **2014**, *80*, 71−79. (c) Liu, Z.; Liu, J.; Zhang, L.; Liao, P.; Song, J.; Bi, X. Silver(I)-Catalyzed Hydroazidation of Ethynyl Carbinols: Synthesis of 2-Azidoallyl Alcohols. *Angew. Chem., Int. Ed.* **2014**, *53*, 5305−5309. (d) Song, Q.-W.; He, L. Robust Silver(I) Catalyst for the Carboxylative Cyclization of Propargylic Alcohols with Carbon Dioxide under Ambient Conditions. *Adv. Synth. Catal.* **2016**, *358*, 1251−1258. (e) Canseco-González, D.; Rodríguez-Victoria, I.; Apan-Ramírez, T.; Viviano-Posadas, A. O.; Serrano-García, J. S.; Arenaza-Corona, A.; Orjuela, A. L.; Alí-Torres, J.; Dorazco-González, A.; Morales-Morales, D. Facile, Single-Step Synthesis of a Series of D-Ring Ethisterones Substituted with 1,4−1,2,3-Triazoles: Preliminary Evaluation of Cytotoxic Activities. *ChemMedChem* **2023**, *18*, No. e202200659.
(40) (a) Savignac, M.; Jaouen, G.; Rodger, C. A.; Perrier, R. E.; Sayer, B. G.; McGlinchey, M. J. Organometallic Derivatives of Hormonal Steroids: 500-MHz One- and Two-Dimensional NMR Spectra of 17$\alpha$-Propynylestra-1,3,5(10)-triene-3,17$\beta$-diol and Its $Co_2(CO)_6$ and $(C_5H_5)_2Mo_2(CO)_4$ Complexes. *J. Org. Chem.* **1986**, *51*, 2328−2332. (b) Osella, D.; Dutto, G.; Jaouen, G.; Vessieres, A.; Raithby, P. R.; De Benedetto, L.; McGlinchey, M. J. Modification of Estradiol at the 17-Position. Effect of Changing the OH Group for a Transition-Metal Carbonyl Cluster on the Estradiol Receptor Recognition. *Organometallics* **1993**, *12*, 4545−4552. (c) Stockland, R. A., Jr.; Kohler, M. C.; Guzei, I. A.; Kastner, M. E.; Bawiec, J. A., III; Labaree, D. C.; Hochberg, R. B. Organometallic Complexes Containing 17-Ethynyl-17$\beta$-hydroxyandrost-4-en-3-one and Related Ethynyl Steroids. *Organometallics* **2006**, *25*, 2475−2485. (d) Cadierno, V.; Conejero, S.; Gamasa, M. P.; Gimeno, J.; Rodríguez, M. A. Activation of Propargylic Alcohols Derived from Hormonal Steroids by the Indenyl-Ruthenium(II) Complex $[RuCl(\eta^5\text{-}C_9H_7)(PPh_3)_2]$: Experimental and Theoretical Evidence of an Allenylidene-Vinylvinylidene Equilibrium. *Organometallics* **2002**, *21*, 203−209. (e) Buil, M. L.; Esteruelas, M. A.; Garcés, K.; Oñate, E. Osmium-Alkenylcarbyne and -Alkenylcarbene Complexes with an Steroid Skeleton: Formation of a Testosterone Organometallic Derivative Containing the 7H-Amino Adenine Tautomer. *Organometallics* **2009**, *28*, 5691−5696.
(41) Su, L.; Dong, J.; Liu, L.; Sun, M.; Qiu, R.; Zhou, Y.; Yin, S.-F. Copper Catalysis for Selective Heterocoupling of Terminal Alkynes. *J. Am. Chem. Soc.* **2016**, *138*, 12348−12351.


https://doi.org/10.1021/acscatal.4c00264
*ACS Catal.* 2024, 14, 8389−8404